

2008

Testing the role of [beta]2-tubulin protein identity on sperm tail axoneme generation and function

Ryan Todd Posgai
University of Dayton

Follow this and additional works at: https://ecommons.udayton.edu/graduate_theses

Recommended Citation

Posgai, Ryan Todd, "Testing the role of [beta]2-tubulin protein identity on sperm tail axoneme generation and function" (2008). *Graduate Theses and Dissertations*. 4986.
https://ecommons.udayton.edu/graduate_theses/4986

This Thesis is brought to you for free and open access by the Theses and Dissertations at eCommons. It has been accepted for inclusion in Graduate Theses and Dissertations by an authorized administrator of eCommons. For more information, please contact mschlange1@udayton.edu, ecommons@udayton.edu.

TESTING THE ROLE OF β 2-TUBULIN PROTEIN IDENTITY ON
SPERM TAIL AXONEME GENERATION AND FUNCTION

Thesis

Submitted to

The College of Arts and Sciences of the

UNIVERSITY OF DAYTON

In Partial Fulfillment of the Requirements for

The Degree

Master of Science in the Department of Biology

by



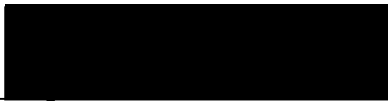
Ryan Todd Posgai

UNIVERSITY OF DAYTON

Dayton, Ohio

August, 2008

APPROVED BY:


Mark G. Nielsen, Ph.D.
Faculty Advisor
Jayne P. Robinson, Ph.D.
Chair, Department of Biology
Sudhindra R. Gadagkar, Ph.D.
Faculty Committee Member

ABSTRACT

TESTING THE ROLE OF β 2-TUBULIN PROTEIN IDENTITY ON SPERM TAIL AXONEME GENERATION AND FUNCTION

Posgai, Ryan Todd
University of Dayton

Advisor: Dr. Mark G. Nielsen, Ph.D.

One of the enduring questions in biology is understanding how proteins evolve while maintaining their function. In *Drosophila melanogaster*, the protein β 1-tubulin is responsible for all somatic cell related microtubule functions, including axoneme assembly in immotile sensory cilia. In the testes, *D. melanogaster* uses β 2-tubulin, a testis-specific isoform of β -tubulin, for axoneme assembly of the motile sperm tail flagellum. Though β 1 and β 2-tubulin are 98% similar in amino acid sequence, differing in only 25 out of a total of 446 amino acids, β 1 cannot assemble a motile axoneme. My research seeks to identify the specific residues that confer upon β 2 its distinctive function. By making small changes in the β 2-tubulin protein sequence and observing the consequences on the structure and function of the sperm tail and axoneme, key amino acids underlying its specialized function can be identified. To achieve this, chimeric β 1/ β 2-tubulin genes containing β 2 identity in the first and third domain (the latter shown to be necessary for assembly of the motile axoneme) of the protein, and β 1 identity in the second domain were constructed, to determine if additional specializations of the β 2 protein resides in the first domain. The efficacy of these chimeras to construct an axoneme and functional sperm tail is currently being tested.

TABLE OF CONTENTS

ABSTRACT.....	iii
LIST OF ILLUSTRATIONS.....	v
LIST OF TABLES.....	vii
CHAPTER	
I. PREFACE AND REVIEW OF THE LITERATURE.....	1
Preface.....	2
Axoneme.....	4
Microtubules.....	6
Dynamic Instability.....	8
Intraflagellar Transport.....	10
Tubulin.....	10
II. TESTING THE ROLE OF β 2-TUBULIN PROTEIN IDENTITY ON SPERM TAIL AXONEME GENERATION AND FUNCTION.....	14
Introduction.....	15
Methods.....	17
Results.....	31
Discussion.....	34
Conclusions.....	38
III. DEVELOPMENT OF A NANOPARTICLE TOXICITY ASSAY USING <i>DROSOPHILA MELANOGASTER</i> AS A MODEL ORGANISM.....	11
Introduction.....	40
Methods.....	43
Results.....	45
Discussion.....	46
Conclusions.....	48
IV. REFERENCES.....	49

LIST OF ILLUSTRATIONS

1.	Schematic representation of the ground plan of a pterygote insect flagellosperm and its ultrastructure.....	53
2.	Illustration of the axoneme with accessory structures.....	54
3.	Intraflagellar Transport.....	55
4.	α and β monomers and heterodimers combine to form protofilaments.....	56
5.	Dynamic instability.....	57
6.	Timeline of the identification of members of the tubulin superfamily.....	58
7.	Phylogeny of all of the Dipteran and Lepidopteran species for which β 2-tubulin has been sequenced.....	59
8.	(A) Electron micrograph of an axoneme from a fertile male with two copies of wild-type copies of β 2; (B) Electron micrograph of an axoneme from a sterile male with two copies of β 1 in place of β 2.....	60
9.	β 1 vs. β 2 amino acid sequences, highlighting the 3 functional domains and the 25 amino acid differences between them.....	61
10.	pBluescript II KS/SK (+) vector into which β 1 β 2C sequence was inserted.....	62
11.	Template β 1- β 2 tubulin chimeric gene, β 1 β 2C.....	63
12.	pCaSpeR IV vector used to insert the β 1- β 2 chimeric gene into the <i>Drosophila</i> germline.	64
13.	Comparison of the nucleotide binding domain, amino acids 1-205, sequence of β 1 and β 2 tubulin.....	65
14.	Comparison of the drug binding domain, amino acids 206-381, of β 1 and β 2 tubulin....	66
15.	Location of <i>Pst</i> I enonuclease restriction enzyme cut sites in pBlueScript II SK+ in relation to the two possible orientations of the chimeric β 1- β 2 insert.....	67
16.	Location of <i>Eco</i> 0109I enonuclease restriction enzyme cut sites in (A) pCaSpeRIV + β 1 β 2C and (B) pCaSpeRIV + β 2 β 1 β 2.....	68

17.	<i>PstI</i> restriction digest of pBlueScript II SK+ $\beta 1\beta 2C$ mutagenesis reaction.....	69
18.	Fifty-nine base pair intron sequence located between Met 73 and Asp 74 of $\beta 1\beta 2C$	70
19.	Agarose gel analysis of five potential new sources of $\beta 1\beta 2C$ to replace the previous intron containing $\beta 1\beta 2C$ insert.....	71
20.	<i>EcoRI</i> digest of pCaSpeRIV + $\beta 1\beta 2CII$ and pBlueScript II SK+ containing the original $\beta 1\beta 2CII$ + intron insert.....	72
21.	<i>EcoRI</i> restriction digests confirming successful ligation of pBlueScript II SK+ DNA - $\beta 1\beta 2CII$	73
22.	<i>EcoRI</i> digest of pCaSpeRIV + $\beta 1\beta 2CII$ and pBlueScript II SK + $\beta 2\beta 1\beta 2$ insert.....	74
23.	Quick PCR screening method.....	75
24.	<i>PstI</i> restriction endonuclease digest of pCaSpeRIV + $\beta 2\beta 1\beta 2$ ligation.....	76
25.	(A) <i>Eco0109I</i> restriction endonuclease digest of pCaSpeRIV + $\beta 2\beta 1\beta 2$ ligation. (B) Positive control (indicated by the star and arrow). <i>Eco0109I</i> digest of pCaSpeRIV + $\beta 1\beta 2C$ shows three bands, as expected.....	77
26.	Second domain mutagenesis of $\beta 1\beta 2C$ in pCasper.....	78
27.	Quick PCR colony screening of pCaSpeRIV + $\beta 2\beta 1\beta 2$ ligation.....	79
28.	<i>EcoRI</i> digest of pCaSpeRIV + $\beta 1\beta 2\beta 2$	80
29.	(A) <i>Drosophilid</i> spiracle openings. (B) Illustration of spiracle opening and branching of the insect tracheal system. (C) Scanning electron microscopic image of <i>Drosophila</i> spiracle.....	81
30.	Minimate compressor, model #PM5, Precision Medical, INC. Northampton, PA.....	82
31.	Filter paper exposed to aerosolized 24 nm Fluospheres.....	83
32.	TEM image of nebulized silver nanoparticles.....	84

33. (A) Negative control. Fly exposed to nebulized water only. (B) Fly exposed to 50µg/mL nebulized CdSe/ZnS quantum dots for five minutes.....85

LIST OF TABLES

1. Nucleic acid and corresponding amino acid sequences of mutagenic primers for 1st (nucleotide binding) domain: primers 1-6, and 2nd (drug binding) domain: primers 7-9.
.....86
2. Forward and reverse, non-mutagenic, β 1 primers designed to sequence the internal regions of the tubulin gene after site-directed mutagenesis.....87

Chapter I.

Preface and Review of Literature

Preface

There are two prerequisites to Dr. Charles Darwin's syllogism of evolution by natural selection:

1. There is variation among phenotypes, and this variation is heritable.
2. Phenotypic selection occurs as a result of differences in the fitness between varying phenotypes.

If either of these two premises fails to hold true, evolution, as driven by natural selection, cannot occur.

The scientific study of evolution has traditionally focused on the latter of the two premises. Population genetics assumes the first premise to be a given and that change, or lack of change, in a phenotype observed over time is, by logic, a result of selection. In the great majority of cases, this does hold true. Many genes of metabolic enzymes have multiple alleles within a population at one time. In *Colias eriphyle*, there are 6 alleles of PGI (phosphoglucose isomerase), all of which convert glucose-6-phosphate into fructose-6-phosphate (Watt *et al.* 1985). This demonstrates both the malleability of the PGI phenotype, as well as serving as affirmation of the paradigm of population genetics.

What if a change in phenotype is not observed over a long period of time? This is not unprecedented. There is very little inter- or intra-specific variation among histone homologs (Graur and Li 2001). This lack of variation is attributed to their fundamental importance in even the most basic biological functions. The same argument cannot be made for the Dipteran testis specific β -tubulin, however. β 2-tubulin amino acid sequence has not evolved in over 60 million years of Dipteran evolution (Fig. 10). Importantly, in contrast to histones, β 2-tubulin is evolving

rapidly in Lepidopteran, the sister clade of Dipterans (Nielsen *et al.* 2006). Unlike histones, $\beta 2$ -tubulin serves as a good candidate to study this question of selection vs. constraint because mutations are not lethal, and resulting phenotypes are recoverable because only the testis tissue is affected. So why hasn't $\beta 2$ -tubulin evolved in Dipterans? Is it because it is the *best* version or is it because it is the *only* version possible. In other words, it is quite possible that selection is not even an option in the Dipteran $\beta 2$ -tubulin because there is zero functional variation available for it to select upon.

Review of Literature

Axonemes

Axonemes are cellular organelles structures that provide motility to cilia and flagella. They support motile cell types (i.e., sperm cells) and allow for movement of fluids (mucus or water) over the surface of cells. In addition, non-motile cilia function as sensory organelles, for example, the non-motile cilia of kidney epithelial cells act as mechano-sensors for fluid flow through kidney tubules. Motile axonemes require a specialized beta tubulin isoform to support their microtubule scaffolding. My research focuses on the structure/function relationship between the *Drosophila* testis-specific beta tubulin, $\beta 2$, and the motile spermtail axoneme. I will begin with a review of axoneme structure and function, followed by a discussion of microtubule assembly and the role of $\beta 2$ tubulin in assembly of the unusually long *Drosophilid* spermtail axoneme.

The axoneme is the core structure of a cilium or flagellum. It is built on a $9 + 2$ array of microtubules in addition to more than 250 accessory proteins (Dutcher, 1995). The $9 + 2$ ultrastructure consists of a set of nine doublet microtubules, each of which consists of a partial B microtubule connected to a complete A microtubule, arranged cylindrically around a pair of singlet microtubules, called the central pair (Fig. 2). The A subtubule, as well as, the central tubules contain 13 protofilaments each. The B subtubule contains 10 protofilaments along with a smaller additional filament (Dallai & Afzelius, 1990). The $9 + 2$ organization of the microtubules allows the sliding of the microtubule doublets against one another to "bend" the cilia or flagella (Warner and Satir, 1974).

The microtubules are arranged with their plus ends at the tip of the axoneme and their minus ends anchored in basal bodies in the cell. Axonemal dynein motors and radial spokes are distributed along each doublet as inner and outer rows of arms. Dyneins are microtubule-dependent force-generating ATPases. The dynein arms act as a bridge between adjacent doublet microtubules, alternately binding and releasing the microtubules in an ATP-dependent manner (Gibbons, 1981). The central pair of microtubules and the radial spokes form a complex and the rotation of this complex during ciliary and flagellar beating acts as a distributor, regulating the activity of the dynein arms (Omoto *et al.*, 1999). The sliding mechanism itself is driven by the ciliary dynein motor protein that is attached to the A sububule of the outer doublets in the form of two dynein arms: the inner and outer dynein arm. The dynein arms connect neighboring doublets in the presence of magnesium and ATP. Acting as an ATPase, the dynein molecules change their conformation and generate a force that leads to the sliding motion of the doublets. The microtubule doublets slide distally to each other using the energy provided by the hydrolysis of ATP, resulting in motion of the flagella.

A feature unique to the insect sperm axoneme is that the ring of nine microtubular doublets is surrounded by nine accessory tubules. The accessory tubules, which originate as outgrowths from the B sububule during spermatogenesis, resemble conventional microtubules (Dallai & Afzelius, 1993). The number of their protofilaments, however, varies between 13 and 20, depending on the taxa. Neighbouring accessory tubules are interconnected with each other and with the adjacent doublet by intertubular material.

Motile cilia and flagella are typically composed of microtubules connected to the plasma membrane arranged in a 9 +2 formation, however, in the evolution of some insect taxa, divergence from the conventional 9 + 2 pattern is quite significant (Dallai *et al.*, 2006) or has

been lost altogether resulting in flagella-less or immotile sperm (Morrow, 2004). Also, there is deviation from this rule among immotile cilia with replacement of the two central microtubules by a single solid core or by 1, 3, or 7 microtubules (Warner, 1972).

Microtubules

Microtubules are involved in several basic cellular processes, including segregation of genetic material, intracellular transport, maintenance of cell shape, positioning of cell organelles, extracellular transport by means of cilia, and movement of cells by means of flagella and cilia. Microtubules can be characterized as long hollow cylinders with outer diameters between 20 nm and 30 nm and an inner diameter of about 16 nm (Bray *et al.*, 1983). In the microtubule, $\alpha\beta$ -tubulin heterodimers bind head to tail into protofilaments, and 13 protofilaments associate in parallel giving rise to a polar cylindrical polymer with a growing (+) end crowned by β tubulin and a shrinking (-) end initiated by α tubulin (Fig. 4). Microtubules can switch stochastically between growing and shrinking phases, both *in vivo* and *in vitro*, a phenomenon known as dynamic instability. This dynamic character is essential to microtubule function (Mitchison and M. Kirschner, 1984).

Assembly and elongation

Microtubule assembly originates in an area near the nucleus known as the Microtubule Organizing Center (MTOC). The minus end of the microtubule is the anchor point in the MTOC. The plus end is the end that binds the GTP molecules that becomes hydrolyzed to GDP when microtubules shrink. Microtubule assembly requires the action of a third type of tubulin, gamma-tubulin (γ -tubulin). The γ -tubulin combines with several other associated proteins to

form a circular structure known as the γ -tubulin ring complex (γ -TuRC). This complex acts as a scaffold for alpha-beta ($\alpha\beta$) tubulin heterodimers to begin polymerization (Oakley *et al.*, 1990). It also acts as a cap of the minus end while microtubule growth continues towards the plus direction. This process of nucleation also requires magnesium and GTP, and it proceeds at 37°C. This stage is relatively slow until the microtubule is initially formed. During nucleation, an alpha (α) and a beta (β)-tubulin molecule join to form a heterodimer, which then assembles into protofilaments. Each heterodimer carries two GTP molecules. The cell consumes energy to keep the concentration of GTP-tubulin high above the critical concentration for polymerization, far from equilibrium, so that subunits rapidly associate with microtubule ends and the microtubules grows. After subunits are incorporated into a microtubule, their GTP is hydrolyzed into GDP, releasing energy. The GDP-bound tubulin depolymerizes the microtubule by curling up protofilaments at its plus end and pulling it apart (Nogales and Wang, 2006).

Polymerization and Depolymerization

Both α and β bind a molecule of GTP. The GTP on α is non-exchangeable, (not hydrolyzed) but is exchangeable on β . After the $\alpha\beta$ heterodimer is added to the growing end of the microtubule, the GTP on β is hydrolyzed to GDP. Hydrolysis occurs when the next subunit is added and α binds to the exposed β . This changes the conformation of the + end of the microtubule, and decreases the strength of the lateral contacts between protofilaments. When polymerization is occurring rapidly, the subunits are being added to the tip faster than the GTP they carry can be hydrolyzed. This maintains a GTP cap on the end of the microtubule. The GTP cap stabilizes the growing microtubule by strengthening lateral interactions, thus preventing depolymerization (McNally, 1999). Occasionally, the GTP molecule at the end will hydrolyze

before the next subunit is added. GDP is now exposed and the microtubule is destabilized. Depolymerization occurs and the microtubule begins to shrink rapidly. This is also known as catastrophe. The GDP-bound tubulin subunits join the free tubulin pool in the cytosol, and exchange the GDP for GTP. They are then ready to be assembled into another growing microtubule.

Dynamic Instability

The growing ends of microtubules are in a constant flux of elongation and retreat. The ceaseless process of polymerization and depolymerization of the protofilament fiber tips that constitute the microtubules has descriptively been compared to “the writhing snakes of Medusa's hair” (Frauss, 2005). This description fits the observations made by researchers Eva Nogales and Hong-Wei Wang. Through the use of cryo-electron microscopy, they revealed at molecular level the forms taken by transitional structures of tubulin during the assembly and disassembly of microtubules. During this process tubulin protofilaments peel away from the end of the microtubule, much like the carvings of wood (Fig. 5) (Nogales and Wang, 2006).

There are a number of proteins known to regulate microtubule polymerization dynamics. They work by stabilizing or destabilizing the + end of the microtubule. Some of the known destabilizing proteins include Kinesin-13, stathmin/OP18, and katanin while some of the known microtubule stabilizing proteins are EB1 and microtubule associated proteins (MAPs), such as XMAP215. (Kinoshita *et al.*, 2001; Moores and Milligan, 2006; Samsonov *et al.*, 2004).

XMAP215 is a member of the class of microtubule binding proteins called +TIPs. +TIPs associate selectively with the growing plus ends of microtubules. These proteins have been shown to be vital in the catalysis of microtubule growth both through enhanced nucleation as

well as polymerization at the + ends (Brittle and Ohkura, 2005; Rogers *et al.*, 2002; Kerssemakers *et al.*, 2006; Kinoshita *et al.*, 2001).

Intraflagellar transport (IFT)

Cilia and flagella are assembled from specialized groupings of microtubules called basal bodies. Axoneme assembly requires that proteins synthesized in the cell body travel to the growing tip of the axoneme, which is distant from their source. This occurs through a process called intraflagellar transport (IFT) and involves motor proteins and protein-carrying vesicles called rafts (Fig. 3). IFT is the bi-directional movement of large protein-containing particles, or “rafts”, along the flagellum in the space between the axoneme and flagellar membrane (Kozminski *et al.*, 1993).

Studies done in *Chlamydomonas*, *Tetrahymena*, *Caenorhabditis elegans*, echinoderms, and mouse show that kinesin-II is the motor protein that mediates IFT (Kozminski *et al.*, 1993; Nonaka *et al.* 1998, Takeda *et al.*, 1999). Kinesin-II is a heterotrimeric kinesin that contains two unique motor subunits from the KIF3A/3B or KRP85/95 kinesin subfamily (Yamazaki *et al.*, 1996). These two subunits associate with a nonmotor subunit called kinesin-associated polypeptide (KAP3) and help regulate the binding of the rafts (Yamazaki *et al.*, 1996).

While kinesin-II regulates the anterograde transport, another motor protein, cytoplasmic dynein 1b, regulates the retrograde transport of axoneme proteins back to the flagellar base, for growth or maintenance (Fig. 2) (Porter *et al.*, 1999). Studies of *C. elegans* (Signor *et al.* 1999) show that kinesin-II can also be cargo. It is shuttled back to the basal body by cytoplasmic dynein 1b during retrograde IFT. By this logic, it stands to reason that cytoplasmic dynein 1b is

carried by kinesin-II to the tip of the flagella, but this still remains to be seen (Porter *et al.*, 1999).

While kinesin-II mediates IFT in a number of organisms, it is not used in assembly of the motile *Drosophila* spermtail axoneme. Studies by Han *et al.* (2003) show that while mutations in kinesin-II disrupt the assembly of the non-motile sensory cilia found in chortodonal organs, they have no effect on the motile, spermtail axoneme. This indicates that *Drosophila* spermtail axoneme morphogenesis does not require IFT. There are two possible reasons for this. The first is that during spermatogenesis spermatids are not enclosed by individual plasma membranes. Rather there is one cytoplasm for all cells, and therefore the growing tip of the axoneme is accessible from the cytoplasm (Fuller 1993; Han *et al.*, 2003). Second, *Drosophila* spermtails are extremely long, from 2.0 mm in *D. melanogaster*, to over 5 cm in *D. bifurca* (Pitnick *et al.*, 1995). The components of IFT may not be able to travel this far and so another, as yet unknown, mechanism may have evolved to support this structure.

Tubulin

There are eight known members of the tubulin super family, they are: alpha (α), beta (β), gamma (γ), delat (δ), epsilon (ϵ), eta (η), zeta (ξ), and iota (ι) (Fig. 6). α , β , and γ -tubulin are present in every eukaryotic organism that has been examined. Unlike α , β , and γ -tubulin, the other tubulins are not ubiquitous among all eukaryotes and are not found in the completed genome sequences of yeast, fungi, higher order plants, and Drospholids (Dutcher, 2003). α , β , and γ -tubulin are all essential proteins. Only one of the other 5 newly discovered tubulin, ϵ , appears to be essential. Mutation or depletion of ϵ -tubulin indicate that they play a role in the proper duplication and assembly of centrioles (Chang *et al.*, 2003).

The three-dimensional structures of α and β are nearly superimposable with only minor differences in the length of some loops and the location of side chains and secondary structures (Nogales *et al.* 1998, 1999). The general three-dimensional structure consists of 2 β -sheets of 6 and 4 strands flanked by 12 α -helices. Functionally, the structure can be divided into three domains: The amino terminal (N-terminal) nucleotide, GTP-binding, domain, the intermediate or drug-binding domain, and the carboxyl terminal (C-terminal) domain, which is the binding site for MAPs and motor proteins (Nogales *et al.*, 1998).

The Rossman fold-containing, N-terminal domain, consists of amino acids 1-205 (Nogales *et al.*, 1998). The Rossman fold is characteristic of nucleotide binding proteins and consists of parallel β strands alternating with α helices. Not surprisingly, this domain is important in forming longitudinal contacts along protofilaments. Also within the N-terminal domain lies the internal variable region (IVR) of β -tubulin. The IVR consists of amino acids 55-57 and is important in the attachment of outer dynein arms (Raff *et al.* 2008).

The drug-binding domain consists of residues 206-381. It is so named because the chemotherapeutic drug Taxol is known to interact within a specific site in this domain. Taxol-type drugs are important antitumor agents used clinically in the treatment of cancers such as: ovarian, lung, breast, and others. It is a combination of β -sheet (S7-S10) and 3 contiguous helices (H8-10) (Nogales *et al.*, 1998). The structures within this domain contain the least conserved sequences between α and β . Consequentially, this explains the differences in dynamic instability between the two tubulin dimers.

The C-terminal domain consists of amino acids 382-446. It contains two anti-parallel helices, H11 and H12, which spread over the surface of the other domains and form the outer covering of the microtubule (Nogales *et al.*, 1998). They are known to be the site of post-

translational modifications and the binding site of MAPs and a range of motor proteins (Nogales *et al.*, 1998). The H11 and H12 connecting loop is involved in the interaction between tubulin monomers along the protofilament (Nogales *et al.*, 1998).

Testis-specific β tubulin and *Drosophilid* spermtail axoneme function

In *D. melanogaster*, there are 5 isoforms of β -tubulin (Rubin *et al.*, 2001). The two isoforms of concern for this research are the “generalist” β 1-tubulin and the “specialist” β 2-tubulin. β 1 is often referred to as the “work horse” tubulin because it is utilized throughout the fly life cycle in almost all tissues, but it is only expressed in the male germ line in the early pre-meiotic stages of spermatogenesis. β 2 is expressed exclusively in the male germ line and is the only β -tubulin utilized in the post-mitotic stages of spermatogenesis (Kemphues *et al.*, 1982). Thus, β 2 can be utilized in the construction of all general categories of microtubules, but is the only version utilized in the assembly of 9 + 2 motile axonemes in the fruit fly.

There is experimental evidence suggesting that β 2 is the only way to make a *Drosophila* axoneme. Manipulation of the expression patterns of β 1 and β 2 have found that other β -tubulin isoforms, even those that are remarkably similar, could not replace β 2 function in the axonemes of motile cilia (Raff *et al.*, 1997; Nielsen *et al.*, 2001).

Much of the study of the functional differences between β 1 and β 2 involve the C-terminus. All tubulins involved in the construction of 9 + 2 axonemes of motile cilia share a conserved sequence within their C-terminal tail (CTT), amino acids 432-446, known as the “axoneme motif” (Raff *et al.*, 1997). A fully CTT-truncated β 2 (β 2 Δ C) was able to assemble spindles and cytoplasmic microtubules, but not axonemes (Nielsen and Raff, 2002). Fusion of the β 2 CTT on to the body of either β 1 or β 3 restored the ability of constructing the 9 + 2

axoneme ultrastructure, but did not fully restore function (Hoyle *et al.*, 1995; Nielsen *et al.*, 2001).

Other potentially important amino acid differences have also been tested. Unexpectedly, addition of $\beta 2$ identity at Thr55 and Ala57, makes $\beta 1$ less able to support an axoneme. This result is in contrast to the additive effects on functionality observed from every other tested chimeric version of $\beta 1$ - $\beta 2$. Decrease of functionality as a result of the addition of Thr55 and Ala57 indicates that there are other, $\beta 2$ -specific, interactions with these two proteins that are necessary for proper $\beta 2$ function. The discovery of this synergistic relationship makes it difficult to continue the study of $\beta 2$ in an additive manner.

Chapter II.

Testing the Role of β 2-tubulin Protein Identity on Sperm Tail Axoneme Generation and Function

Introduction

Axoneme morphogenesis in *Drosophila* provides a unique model to study the role of structure/function relationships in protein evolution. In *Drosophila melanogaster*, the protein β 1-tubulin supports microtubules and spindles in the embryo throughout development and is used for axoneme assembly in all cells except for those of the testes (Kaltschmidt *et al.*, 1991).

In the testes, *D. melanogaster* uses the β 2-tubulin, a testis specific isoform of β -tubulin, for all microtubule related functions, including assembly of the sperm tail flagellum. β 1 and β 2-tubulin are 98% similar in amino acid sequence, differing in only 25 out of a total of 446 amino acids (Rudolph *et al.*, 1987, Michiels *et al.*, 1987). However, this slight difference between the two proteins has a remarkable effect on their ability to construct functional sperm tail flagellum (Raff *et al.*, 2000). β 2-tubulin assembles fully functional sperm tail flagellum (Fig. 11A). When β 2 is replaced with β 1-tubulin in the testes, or chimeric β 1- β 2 tubulins up to 99% similar in identity, proper axoneme assembly does not occur, resulting in a short, non-functional sperm tail (Fig. 11B) (Raff *et al.* 2000; Nielsen *et al.* 2001). Further, a synergism was identified, which reveals that further testing one at a time will not be reasonable.

The above results are the crux of β -tubulin research in *Drosophila*. How can two such similar proteins be so incompatible in function? In order to begin to answer these questions, it is necessary to identify axoneme specific amino acid sequences in β 2. This project is a continuation of the above-described research. β -tubulins contain three functionally distinct protein domains: the nucleotide-binding domain, drug-binding domain, and the carboxyl terminus. β 1 and β 2-tubulin amino acid sequence differ slightly in all of these regions. To

determine where $\beta 2$ function resides, changes can be made in each of these regions to determine which, if any, is most important in the proper generation and function of the sperm tail axoneme.

Much is known about the functional significance of the amino acid differences of the carboxyl terminus. However, there is considerably less known about the amino acid differences in the other two domains. This project tests the effects of changing $\beta 1$ sequence identity to $\beta 2$ identity in both the nucleotide-binding region and the drug-binding region in addition to the already constructed and tested carboxyl terminus. At the end of my project, each individual domain will have been tested. This process will help identify any of the 16 amino acid differences in the nucleotide and drug binding domains that may be synergistically important to the amino acid differences in the carboxyl terminus.

If the evolution of the current amino acid sequence of $\beta 2$ is path dependent, it is possible that no combination of the 25 differences between $\beta 1$ and $\beta 2$ is sufficient to restore full axoneme functionality to $\beta 1$ and that only the exact amino acid identity of $\beta 2$ will suffice. Because it is impossible to test $25!$ combinations of amino acid differences, the results of this experiment may significantly reduce that number to one that is much more manageable, even if it is never exhaustively testable.

If it is found that neither the nucleotide- nor drug- binding domains in combination with the C-terminal domain restore $\beta 2$ functionality, this would suggest that $\beta 2$ function is a result of complex interactions between the amino acids of all of the domains. However, if it is found that a certain domain does take precedence in sperm tail axoneme formation, then it may be possible to locate the exact amino acids that are responsible for the functional specificity of $\beta 2$.

Methods

The Vectors

The vector used as the template for site-directed mutagenesis was pBlueScript II SK+ (Stratagene) (Fig. 10). pBlueScript II SK+ is an approximately 3 kb phagemid. A phagemid is a hybrid cloning vector of the filamentous phage M13 and a plasmid to produce a vector that can be propagated like a plasmid. pBlueScript II SK+ contains an *E. coli* fl helper phage origin of replication (ORI) gene, an ampicillin antibiotic resistance sequence, and a multiple cloning site (MCS) with a single *EcoRI* restriction cut site into which our chimeric $\beta 1$ - $\beta 2$ tubulin gene is inserted. This $\beta 1$ - $\beta 2$ chimera is essentially the $\beta 1$ gene replaced with $\beta 2$ amino acid sequence identity within the carboxy terminal region, codons 433-434, 437, 439-440, and 442-444 (Fig. 11). This specific chimera is referred to as $\beta 1\beta 2C$. Following the mutagenesis of all first domain sites of $\beta 1\beta 2C$ to $\beta 2$ identity the chimera is referred to as $\beta 2\beta 1\beta 2$ and following the mutagenesis of all second domain sites of $\beta 1\beta 2C$ to $\beta 2$ identity the chimera is referred to as $\beta 1\beta 2\beta 2$.

pCaSpeRIV was used as the transformation vector (Fig. 12). pCaSpeRIV is a 7855 base-pair non-autonomous P-element vector which allows transposition of the chimeric gene into the fly genome. A P-element vector is a 2907-bp class II transposon that is widely believed to have originated in the Drosophilids within the last 100 years (Kidwell, 1993). pCaSpeRIV contains a single *EcoRI* restriction enzyme cut site into which either the chimeric $\beta 2\beta 1\beta 2$ or $\beta 1\beta 2\beta 2$ genes are cloned. pCaSpeRIV also contains 1.8 kb of 5' and 1.3 kb of 3' $\beta 2$ regulatory sequence flanking the *EcoRI* restriction site, and ultimately, the inserted chimeric $\beta 1$ - $\beta 2$ gene as well (Fig. 12). This regulatory sequence ensures the equivalent *in vivo* expression of the chimeric gene *in*

lieu of the absent $\beta 2$ gene (Hoyle and Raff, 1990). The vector also contains a wild-type version of the white-eye gene to serve as a phenotypic expression marker. In total, the casper vector (7.8kb) + the B2 regulatory sequence (2.8 kb) + the beta tubulin coding sequence (1.3kb) = 11.6kb.

Primer Design

Sets of oligonucleotide primers were designed to change $\beta 1\beta 2C$ tubulin sequence identity to $\beta 2\beta 1\beta 2$ and $\beta 1\beta 2\beta 2$ identities, respectively. The web-based primer design tool, Primer3®, was used to aide in the design of the primers.

Altering the template $\beta 1\beta 2C$ sequence identity to $\beta 2\beta 1\beta 2$ sequence identity required changing the nucleotide sequence coding identity of 12 amino acids within the length of the 205 amino acid nucleotide binding domain (Fig.13). Due to the distance between the amino acid sites requiring mutagenesis, the design of multiple primers was necessary. Mutagenic primer 1 was designed to alter $\beta 1$ amino acid Ala18 to $\beta 2$ Gly18, $\beta 1$ amino acid Ile23 to $\beta 2$ Val23, and $\beta 1$ amino acid Gly29 to $\beta 2$ Cys29 (Table 1). Mutagenic primer 2 was designed to alter $\beta 1$ amino acid His37 to $\beta 2$ Tyr37 (Table 1). Mutagenic primer 3 was designed to alter $\beta 1$ amino acid Ser55 to $\beta 2$ Thr55, $\beta 1$ amino acid Gly57 to $\beta 2$ Ala57, and $\beta 1$ amino acid Val64 to $\beta 2$ Ile64 (Table 1). Mutagenic primer 4 was designed to alter $\beta 1$ amino acid Pro80 to $\beta 2$ Ala80 (Table 1). Mutagenic primer 5 was designed to alter $\beta 1$ amino acid Ala124 to $\beta 2$ Ser124, $\beta 1$ amino acid Ser126 to $\beta 2$ Gly126, and $\beta 1$ amino acid Ser135 to $\beta 2$ Leu135 (Table 1). (The change of $\beta 1$ amino acid Ser135 to $\beta 2$ Leu135 is not really a change from $\beta 1$ identity to $\beta 2$ identity. It was discovered through the process of designing the primers that the original source of the sequence data was incorrect, and that the proper amino acid coding for $\beta 2$ amino acid 135 is indeed Leu,

not Ser). Mutagenic primer 6 was designed to alter $\beta 1$ amino acid Ser163 and Tyr167 to $\beta 2$ Ile and Phe, respectively (Table 1).

Altering the template $\beta 1\beta 2C$ sequence identity to $\beta 1\beta 2\beta 2$ sequence identity required changing the nucleotide sequence coding identity of 4 amino acids within the length of the 175 amino acid drug-binding domain (Fig.14). Again, due to the distance between the amino acid sites requiring mutagenesis, the design of multiple primers was necessary. Mutagenic primer 7 was designed to alter $\beta 1$ amino acid Leu281 to $\beta 2$ Ala281 (Table 1). Mutagenic primer 8 was designed to alter $\beta 1$ amino acids Tyr340 and Val349 to $\beta 2$ Phe and Cys, respectively (Table 1). Finally, mutagenic primer 9 was designed to change $\beta 1$ amino acid Ile381 to $\beta 2$ Val381 (Table 1).

It was also necessary to design internal primers for sequencing purposes. T7 and T3 sites are contained in pBlueScript II SK+® plasmid and flank the insert site. These sites are useful for sequencing the 5' and 3' ends of the insert. However, many of the $\beta 2\beta 1\beta 2$ and $\beta 1\beta 2\beta 2$ mutagenesis sites lie well within the gene and were beyond the capabilities of the plasmid flanking T7 and T3 sites. In order to sequence the full length of the insert two internal primers were designed: RTP1 forward and RTP2 reverse (Table 2).

All of the primers used in this study were ordered from Integrated DNA Technologies, Inc.

Site-Directed Mutagenesis

Multi site-directed mutagenesis was used to change the identities of the target amino acids (QuikChange® Multi site-directed mutagenesis, Statagene). Up to five different sites can be simultaneously targeted for mutagenesis using the QuikChange Multi Site-Directed

Mutagenesis kit. There are three main steps in the one-day procedure. Step 1, a thermal cycling procedure was used to achieve multiple rounds of mutant strand synthesis. The 50 μ L reaction included: 5 μ L 10X reaction buffer (Stratagene), 50 ng of dsDNA template, 125 ng of a combination of up to 5 designed oligonucleotide primers #1-9, 1 μ L of dNTP mix, water to a final volume of 50 μ L, then add 1 μ L of *PfuUltra* HF DNA polymerase (2.5U/ μ L). In step 2 of the procedure, the thermal cycling reaction products were treated with the restriction endonuclease *Dpn* I. *Dpn* I was used to digest any residual non-mutant strand DNA (parental DNA) because it targets methylated and hemimethylated DNA and DNA isolated from *E. coli* strains is dam methylated. Step 3 was the transformation step. XL10-Gold® ultracompetent cells were thawed on ice and 45 μ L of the cells were aliquoted into a pre-chilled BD Falcon® polypropylene round bottom tube. 2 μ L of β -ME mix was added and the tube was incubated on ice for 10 minutes, with swirling every 2 minutes. After 10 minutes, 1.5 μ L of the *Dpn*-I treated DNA was added. The tube was swirled gently to mix and then incubated on ice for 30 minutes. The tube was heat-pulsed in a 42°C water bath for exactly 30 seconds and placed on ice for 2 minutes. Next, 800 μ L of pre-heated (42°C) NZY⁺ broth was added and the tube was incubated at 37°C for 1 hour. 100 μ L of the newly transformed cells were plated on LB ampicillin agar plates (50 μ g/mL) and placed into a 37°C incubator overnight. After 24h, individual colonies were cultured overnight in LB ampicillin (50 μ g/mL) media for plasmid preparation. Within the ultracompetent cells, the mutant closed circle ssDNA was converted into duplex form *in vivo*.

Isolation of DNA and Orientation of the Insert

From the transformed and plated cells, double stranded plasmid DNA, containing the target gene with mutagenized amino acids, was obtained. Approximately, 10 colonies were chosen at random for DNA isolation.

Plasmid DNA was isolated using the QIAGEN plasmid purification system. The 50mL culture was centrifuged at 13,000 x g for 15 minutes at 4°C and the supernatant was removed. The pellet was re-suspended in 4mL of buffer P1 and vortexed until completely re-suspended. Four mL of lysis buffer P2 was added and mixed gently by inversion and allowed to incubate at room temperature for 5 minutes. Next, 4mL of chilled neutralizing buffer P3 was added, mixed gently by inversion, and incubated on ice for 15 minutes. After 15 minutes the mixture was centrifuged at 13,000-x g for 30 minutes at 4°C and the supernatant was removed and placed into a new tube. The supernatant was precipitated using 1/10 the volume of 3M sodium acetate and 2x volume of ethanol. The mixture was then placed in -20°C overnight. The next day the solution was centrifuged for 30 minutes at 20,000 x g at 4°C to pellet the DNA. The supernatant was removed and the pellet was re-suspended in 100µl of water.

For sequencing purposes, it was necessary to know the orientation of the insert within the plasmid. Most of the mutagenesis sites lie in the nucleotide-binding region of the tubulin gene. Knowing whether the insert is positioned 5'→3' or 3'→5' with respect to the flanking T7 and T3 sites allows for maximization of the sequencing process. To do this, the β2β1β2 and β1β2β2 chimeric genes were subjected to restriction endonuclease digestion using *PstI* endonuclease (5µL DNA, 1µl *PstI* enzyme and 4µl 10x buffer [New England BioLabs]). *PstI* has one cut site within pBlueScript II SK+® (as well as pCaSpeRIV) and one cut site within β1 and β2 tubulin

(Fig. 15 & Fig. 16). The position of the *Pst*I cut site in tubulin is between codons 127 and 128 and the position of the cut site in pBlueScript II SK+® is 5' to the insert. With this knowledge, the orientation of the insert can be determined by observing the length of the DNA fraction obtained after digestion. The restriction digest reaction was size-fractionated by agarose gel electrophoresis (1% agarose, 1X buffer TAE at 100 milliamps < 1 hour), stained with ethidium bromide and visualized under UV light (Fig. 17).

Sequencing

The fidelity of the multi site-directed mutagenesis procedure is high, but well below 100 percent. Therefore, the prepped DNA samples were sent to Northwoods DNA, Inc. for sequencing (10µL total volume: 1µg pBlueScript II SK+, 5 µM primer or 10µL total volume: 1.5µg pCaSpeRIV, 5µM primer).

The samples that had the greatest number of successful mutagenesis changes were re-subjected to the multi site-directed mutagenesis procedure, using the mutagenic oligonucleotide primers that failed during the previous attempt, as well as, any additional mutagenic primers that were required to complete mutagenesis of all the $\beta 2\beta 1\beta 2$ or $\beta 1\beta 2\beta 2$ amino acid sites. This process of mutagenesis → sequencing → further mutagenesis was repeated until all targeted sites were successfully changed.

The Intron

During the analysis of one of the first nucleotide sequence chromatograms of the mutagenized $\beta 2\beta 1\beta 2$ and $\beta 1\beta 2\beta 2$ tubulin genes, it was unexpectedly discovered that a 59-nucleotide length intron lay between amino acids 73 and 74 (Fig. 18). This intron caused great

concern and steps were taken to remove it or, alternatively, find a new $\beta 1\beta 2C$ template source gene that did not contain the insert.

In hopes of finding a way to cut the intron out of the gene, candidate restriction endonuclease enzymes that closely flanked the intron site and that were also not found anywhere else within the gene or plasmid were identified. The short list included: *DraII* and *EcoRV*.

The more promising solution was to find another source template of $\beta 1\beta 2C$ that did not contain the intron. Five alternative sources of plasmid $\beta 1\beta 2C$ were obtained and analyzed using agarose gel electrophoresis (1% agarose, 1X buffer TAE at 100 milliamps for < 1 hour), stained with ethidium bromide, and visualized under UV light (Fig. 19). Based on analysis of the gel image, all of the $\beta 1\beta 2C$ sequences were located in pCaSpeRIV.

Gel Extraction and Ligation into pBlueScript II SK+

It was fully believed that the intron found in the initial $\beta 1\beta 2C$ template sequence was an anomaly. Therefore, one of the cleanest-looking of the five alternative sources of insert, from here on referred to as $\beta 1\beta 2CII$, was chosen to be used in lieu of the original $\beta 1\beta 2C$ template (Fig. 19). The $\beta 1\beta 2CII$ insert was located in the transformation vector, pCaSpeRIV. Due to the size of pCaSpeRIV + insert (~9kb), it was not recommended to perform mutagenesis on the insert while it was in this plasmid.

The $\beta 1\beta 2CII$ chimeric gene was extracted from the pCaSpeRIV vector by restriction endonuclease digestion using *EcoRI* (50 μ L DNA, 4 μ L *EcoRI* enzyme and 6 μ L 10x buffer [Promega]). The restriction digest reaction was size-fractionated by agarose gel electrophoresis (1% agarose, 1X buffer TAE at 100 milliamps < 1 hour), stained with ethidium bromide, and visualized under UV light. The 1.7 kb band corresponding to the $\beta 1\beta 2CII$ chimeric gene was

excised out of the gel (Fig. 20). DNA was eluted from the gel using the QIAEX II gel extraction kit (Qiagen). The excised band was weighed and 3 volumes of buffer QX1 was added to the excised piece of gel. Next, 10 μ L of QIAEX II DNA-binding bead suspension was added and the tube was incubated at 50°C for 10 minutes, vortexing every 2 minutes to keep the QIAEX II in suspension. The sample was centrifuged for 30 seconds and the supernatant was removed. The remaining pellet was washed with 500 μ L of buffer QX1 and washed twice with 500 μ L buffer PE. The pellet was allowed to air dry for 15 minutes until the pellet turned white, then 20 μ L of nuclease-free water was added to elute the DNA.

pBlueScript II SK+ vector containing the original β 1 β 2C + intron insert was cut with the *EcoRI* restriction endonuclease enzyme and then treated with Calf Intestinal Alkaline Phosphatase (CIP) (20 μ L pBlueScript II SK+ DNA in water, 2.2 μ L 1xNEBuffer, 0.4 μ L CIP; incubate at 37°C for 1 hour). CIP is an enzyme that catalyzes the removal of phosphate groups from the 5' ends of DNA. The phosphatase treatment was performed to prevent the vector from re-ligating with itself instead of the insert. CIP was inactivated by incubating at 65°C for 30 minutes. The restriction digest reaction was size-fractionated by agarose gel electrophoresis (1% agarose, 1X buffer TAE at 100 milliamps, <1 hour), stained with ethidium bromide, and visualized under UV light. The 3.0 kb band corresponding to the pBlueScript II SK+ plasmid was excised out of the gel (Fig. 20).

The excised β 1 β 2CII DNA sequence was ligated into the CIP-treated pBlueScript II SK+ vector (5 μ L pCaSpeRIV DNA, 3 μ L pBlueScript II SK+ DNA, 1 μ L 10X buffer, 1 μ L T4 DNA ligase [New England Biolabs], room temperature overnight). The pBlueScript II SK+ DNA - β 1 β 2CII ligation reaction was transformed into DH5 α competent cells, plated on LB-ampicillin

plates for blue/white screening. The ligation was not successful until CIP was replaced with Antarctic phosphatase (AP). AP works in much the same way as CIP, but it is less stable at higher temperatures, therefore, its inactivation curve is much steeper and more complete than CIP.

Successful ligation was determined by blue/white screening. Eight white colonies were selected, cultured in LB/ampicillin (50µg/mL) overnight, and isolated using the QIAGEN plasmid purification system. The purified plasmids were digested with *EcoRI* restriction enzyme to check for $\beta 1\beta 2$ CII insert presence (Fig. 21). The 7 samples with inserts were sent to Northwoods DNA, Inc. for sequencing. The sequencing results showed that $\beta 1\beta 2$ CII also contained the 59-nucleotide intron.

A different plasmid containing yet another source of $\beta 1\beta 2$ C was chosen. This time sequencing was performed before ligation was attempted. Once again, the 59-nucleotide intron was located within the $\beta 1\beta 2$ C sequence.

Soon after this latest attempt was sequenced, it was conferred by the original creators of the $\beta 1\beta 2$ C template at Indiana University, that the intron in our sequence was endogenous to the $\beta 2$ -tubulin sequence and its presence was not a cause for concern.

Gel Extraction and Ligation into pCaSpeRIV

With the intron issue resolved, the focus was on getting the $\beta 2\beta 1\beta 2$ and $\beta 1\beta 2\beta 2$ chimeric genes ligated into the transformation vector, pCaSpeRIV.

$\beta 2\beta 1\beta 2$ was excised from pBlueScript II SK+ by restriction endonuclease digestion using *EcoRI* (50µL DNA, 4µL *EcoRI* enzyme and 6µL 10X buffer [Promega]). The restriction digest reaction was size-fractionated by agarose gel electrophoresis, stained with ethidium bromide, and

visualized under UV light. The 1.7 kb band corresponding to the $\beta 2\beta 1\beta 2$ chimeric gene was excised and eluted from the gel using the QIAEX II gel extraction kit (Qiagen) (Fig. 22).

pCaSperIV was also *EcoRI* digested, size-fractionated by agarose gel electrophoresis, stained with ethidium bromide, and visualized under UV light. The 8 kb band corresponding to the *EcoRI* cut pCaSperIV was excised, eluted from the gel using the QIAEX II gel extraction kit (Qiagen), and then Antarctic phosphatase treated (Fig. 22).

The concentration of the DNA was estimated by comparing the brightness of the sample DNA bands with the known amounts of the 1 kb DNA ladder. From this, numerous and varying ratios of insert to vector ligation reactions were set up and incubated at either room temperature, 16°C, or 4°C.

Quick Assay PCR Screening Method

Unlike pBlueScript II SK+, successful ligation identification is not capable by blue/white colony screening in pCaSperIV because it does not contain a Lac operon within the MCS. This is problematic because Antarctic phosphatase is not 100% efficient at removing every single 5' phosphate that allows some ligation, or "re-closing", of the two ends of the cut vector to occur. Because of the lack of blue-white screening and because many of the pCaSperIV + $\beta 2\beta 1\beta 2$ or $\beta 1\beta 2\beta 2$ ligation reactions yielded plates with >25 colonies, identification of successful ligation reactions was laborious, costly, and inefficient.

The initial method of randomly selecting colonies, culturing the bacteria, isolating the DNA, *EcoRI* restriction endonuclease digestion, and agarose gel electrophoresis fractionation soon gave way to a quick PCR screening method. Bacteria colonies were systematically

processed by taking a small sample of the colony, dipping it into a PCR reaction mix containing RTP1 forward and RTP reverse primers, and performing a PCR reaction (Fig. 23).

New Sources of pCaSpeRIV

After numerous unsuccessful ligation attempts using the original stock source of pCaSpeRIV, it was postulated that perhaps the pCaSpeRIV vector was the cause of the problem. Many new sources were located and the most promising ones were chosen for use in lieu of the original pCaSpeRIV source. Some of the new pCaSpeRIV sources contained other previously tested chimeric versions of $\beta 1$ - $\beta 2$ tubulin, and others contained no insert, whatsoever.

Lipofection as an Alternative to Ligation

In the quest to find an alternative solution to the ligation reaction, a new lipofection-based testis protein expression technique being developed in the lab was explored. Lipofection is a technique used to inject material into a cell by means of using liposomes. Liposomes are vesicles that can easily merge with the cell membrane because they are composed of a lipid bilayer.

Virgin male flies were collected and their testes were dissected in TB buffer and transferred in 100 μ L of Grace's Insect Culture Media (Invitrogen). GFP plasmid, pTRACER-EF/BSD and the $\beta 2$ expression vector, pCaSpeRIV were isolated and eluted in deionized water. For each treatment, 5uL of plasmid DNA was allowed to equilibrate in 45uL of Grace's Media for 5 minutes at room temperature. At the same time, 10uL of Lipofectamine 2000 (Invitrogen) was equilibrated in 40uL of Grace's Media for 5 minutes at room temperature. The two solutions were then mixed and allowed to form complexes for 20 minutes at room temperature.

The complexes were then added to the dissected testes and incubated at room temperature for 48 hours. After 48 hours, the testes were then aceto-orcein stained and examined using fluorescence microscopy.

***Eco0109I* Endonuclease Restriction Enzyme as an Improved Screening Enzyme**

PCR colony screening of a pCaSpeRIV + $\beta 2\beta 1\beta 2$ ligation reaction indicated a possible successful ligation reaction. *PstI* restriction digest also provided supporting evidence (Fig. 24). The double bands indicated that the *PstI* enzyme cut twice (once within the pCaSpeRIV vector and once within the $\beta 2\beta 1\beta 2$ insert), and addition of the two band sizes equaled the expected size of a vector with an insert, reaffirming the conclusion of ligation success. However, since 7 of the 9 colonies picked indicated that there was ligation, we took the caution of double checking the results. A restriction enzyme was identified that has a cut site unique to $\beta 1\beta 2C$ and is lost in $\beta 2\beta 1\beta 2$ through the site directed mutagenesis process. Restriction enzyme *Eco0109I* has two cut sites in pCaSpeRIV and recognizes a sequence of DNA at amino acid 80 of $\beta 1\beta 2C$, but does not have a cut site in $\beta 2\beta 1\beta 2$ (Fig. 25B). Therefore, if the apparent insert indicated by the *PstI* digest was truly $\beta 2\beta 1\beta 2$, agarose gel electrophoresis of an *Eco0109I* digest of the same samples should show two bands. If the *Eco0109I* digest results in three pieces of DNA, it would indicate that the insert is an accidental carry-over or contamination of pCaSpeRIV + $\beta 1\beta 2C$.

Right Insert, Wrong Vector

PCR screening of ligation reactions using primer RTP1 again indicated successful ligation of pCaSpeRIV + $\beta 2\beta 1\beta 2$ (Fig. 27). *PstI* and *Eco0109I* restriction digests also reaffirmed the presence of $\beta 2\beta 1\beta 2$. Once again, however, *EcoRI* digestion of the apparent

successful ligation reaction revealed that even though the insert was correct, the vector was not (Fig. 28). The size of the vector was consistent with pBlueScript II SK+. This result indicates that either the ligation ingredients were cross-contaminated with a small amount of pBlueScript II SK+ or some of it was transferred during the gel extraction procedure.

Mutagenesis of $\beta 1\beta 2C$ in pCaSpeRIV

Another attempt to circumvent the ligation step was to perform site-directed mutagenesis on $\beta 1\beta 2C$ in pCaSpeRIV. Stratagene's QuikChange® Multi site-directed mutagenesis kit was used because it is designed to handle mutagenesis on vectors up to 6 kb's. No other mutagenesis kit was found that could handle vectors larger than 6 kb. pCaSpeRIV + $\beta 1\beta 2C$ is an approximately 9 kb vector. Although this size range is well outside of the claimed capabilities of the mutagenesis kit, it was hoped that if the mutagenesis reactions were performed in mass, at least one of them would be successful.

Ethidium Bromide-Free Staining and a Positive Control Ligation

It is known that ethidium bromide can have an inhibitory effect on DNA ligase enzyme (Miyaki, 1971, Aktipis, 1976). To test whether ethidium bromide was inhibiting T4 DNA ligase, we eliminated the ethidium bromide staining step from our procedure. In order locate the samples on the agarose gel without staining, duplicate samples were run along side the samples of interest. After electrophoresis, the gel was cut in half, stained with ethidium bromide, and then laid along side the unstained half of the gel. The location of the unstained and non-visible DNA of interest could then be inferred and extracted from the gel. DNA was successfully

isolated via this method many times, but the results of the ensuing ligation reactions remained the same.

In the continued search for the cause of the failing ligation reactions, a positive ligation control was designed. To test the ability of both the insert and the vector to be ligated, the sources of $\beta 2\beta 1\beta 2$ (in pBlueScript II SK+) and pCaSpeRIV (with $\beta 1\beta 2C$ insert sequence) were *EcoRI* digested to separate each insert from their vectors. The *EcoRI* digests were then agarose gel fractionated, extracted, and the inserts were immediately ligated back into each of their respective source vectors from which they were just extracted.

Results

Orientation of the Insert in pBlueScript II SK+

After agarose gel fractionation of the *Pst*I digests, there are two possible sizes of the small DNA bands: ~0.5 kb or ~1.3 kb. Based on the size of the small DNA band, it was determined that the insert was positioned 5'→3' with respect to the *Pst*I cut site in pBlueScript II SK+ (Fig. 17).

Ligation of Alternative Source of β 1 β 2C into pBlueScript II SK+ & Sequencing

With the discovery of the 59-base intron in the original β 1 β 2C sequence, a new source of β 1 β 2C had to be found. The new source of β 1 β 2C was not located in the mutagenesis vector, pBlueScript II SK+, but it was in the transformation vector, pCaSpeRIV. As a result, β 1 β 2CII had to be cut out of pCaSpeRIV and ligated into pBlueScript II SK+. This process was made easier because of the blue/white colony screening of pBlueScript II SK+. When β 1 β 2CII was successfully ligated into pBlueScript II SK+ and transformed into a competent cell, it produced a distinctive white colony when grown on a LB/amp selective media plate. Once white colonies were observed, they were cultured and DNA was isolated via plasmid preparation. β 1 β 2CII was then sequenced to be certain that it did not contain the 59-base intron. The sequencing results showed that β 1 β 2CII also contained the 59-nucleotide intron (Fig. 18). The same results were obtained when a third source of β 1 β 2C was sequenced.

The process of identification of new sources of $\beta 1\beta 2C$, ligation into pBlueScript II SK+, and sequencing encompassed nearly a six-month period of time. At the end of the six months, it was finally communicated from the people that originally created the version of pCaSpeRIV used for *in vivo* expression of $\beta 2$ -tubulin that the intron that we had found was not a concern.

Gel Extraction and Ligation into pCaSpeRIV

Once the two new chimeras, $\beta 2\beta 1\beta 2$ and $\beta 1\beta 2\beta 2$, were created via mutagenesis in pBlueScript II SK+ and the 59-nucleotide intron was issue was resolved, all that remained before injection into the germ line embryo cells and visualization of the resulting phenotype, was ligation of the insert into the transformation vector, pCaSpeRIV. This step proved to be much more difficult than anyone had ever envisioned, and was ultimately insurmountable. The ligation failed innumerable times, despite various attempts at finding a solution, including: varying the ratio of insert to vector, purchasing all brand new ligation reaction ingredients, incubating at a range of temperatures, and trying different sources of both insert and vector, among others.

Lipofection as an Alternative to Ligation

Considering the problems with the ligation reaction, the possibility of gene expression via lipofection was a promising alternative. The lipofection method proved to be unfruitful, however, and was abandoned after it was shown that dissected testes could not be easily transfected with plasmid DNA via a liposome-mediated reaction.

***Eco0109I* Endonuclease Restriction Enzyme as an Improved Screening Enzyme**

The agarose gel electrophoresis of the *Eco0109I* digests showed two bands (Fig. 25A). This result indicated that the apparent insert was indeed $\beta 2\beta 1\beta 2$. However, subsequent DNA sequencing analysis indicated otherwise. After a number of failed attempts to sequence the insert, a thorough review of the experimental procedure revealed that there are actually two *PstI* cut sites in pCaSpeRIV. This also explains the double band result of the *Eco0109I* digest. The reason that there were only two cut sites (Fig. 25A) was not because the supposed insert's *Eco0109I* cut site had been changed by mutagenesis, but because there wasn't an insert in the vector at all.

Mutagenesis of $\beta 1\beta 2C$ in pCaSpeRIV

The results of mutagenesis of the ~9 kb pCaSpeRIV vector + $\beta 1\beta 2C$ insert showed that while the PCR/mutagenesis reaction appeared to work, the size of the yielded DNA was much smaller than the expected 9 kb (Fig. 26). This result can be explained as a consequence of the large size of pCaSpeRIV + $\beta 1\beta 2C$. The vector was too large for the polymerase to traverse its full length and it subsequently fell off before it replicated the entire vector.

Positive Control Ligation

The positive control ligation experiment, designed to test whether both the chimeric $\beta 1\beta 2$ insert and the pCaSpeRIV vector were even capable of being ligated, was successful for the pBlueScript II SK+ with $\beta 2\beta 1\beta 2$ insert but not successful in the case of pCaSpeRIV + $\beta 1\beta 2C$.

Discussion

Despite an exhaustive effort, ligation of $\beta 2\beta 1\beta 2$ or $\beta 1\beta 2\beta 2$ into pCaSpeRIV was never achieved. The reason, or reasons, for this failure were never fully determined. It often seemed as if one test would indicate one thing only to be confounded, or refuted outright, by ensuing experiments. Also, as if ligation was not a large enough issue, the experiment was often disrupted by false positive results or derailed for extended periods of time by tangential problems, such as, the 59-base intron and incorrect information regarding the number of *PstI* cut sites. The struggles with the ligation were especially frustrating because once the chimeric gene is inserted into pCaSpeRIV, all that is left to do is express the gene *in vivo* and then observe the resulting phenotype.

That said, however, the process of investigating and trouble shooting the sundry of unexpected problems helped in the development and honing of sound research skills, as well as, enlightening some key issues of the research project.

One of the more important areas of enlightenment was the discovery of the 59-nucleotide base intron located between amino acids 73 and 74 of the $\beta 1\beta 2C$ sequence. The original template of $\beta 1\beta 2C$ was $\beta 1$ -tubulin. As mentioned above, $\beta 1$ -tubulin identity only differs from $\beta 2$ -tubulin identity by 25 amino acids, yet it is not capable of replacing $\beta 2$ function in the testes. In order to determine which of the 25 amino acids are most important in conferring $\beta 2$ functionality to $\beta 1$, the $\beta 1$ sequence was being mutated to resemble $\beta 2$. Even more puzzling than the presence of the intron was its identity. A Genbank search revealed that it was a $\beta 2$ -intron sequence. Considering the proven sensitivity of $\beta 2$ to even minor changes to its amino acid sequence (Fackenthal *et al.*, 1995; Nielsen *et al.*, 2001), there was serious concern that the

presence of the intron in the middle of the amino acid coding sequence would have a major effect on its regulation and expression *in vivo*. A review of the literature at the time and attempted contact with the researchers that developed the original version of the investigative model, revealed nothing about the intron's origin or its possible effects.

After lengthy consideration, it was concluded that the intron must have been a complete anomaly that was somehow introduced to that specific $\beta 1\beta 2C$ sequence by sheer chance, or accident, at some near-past time point. The decision was made to use one of the other stocks of $\beta 1\beta 2C$ that would assuredly not contain the intron. This, however, did not turn out to be the case. In all, three different stocks of $\beta 1\beta 2C$ were sequenced and all three contained the intron. Luckily, before the situation prolonged itself any further, communication was finally received from researchers at Indiana University that the intron was endogenous to the $\beta 2$ sequence and it has no effect on *in vivo* regulation or expression.

However, the intron was not the biggest hurdle of the project. Ligation of $\beta 2\beta 1\beta 2$ and $\beta 1\beta 2\beta 2$ sequences into pCaSpeRIV was, ultimately, an insurmountable obstacle.

The specific ligation reaction of concern to this project was made even more difficult than the typical ligation reaction because of the lack of blue/white colony screening and the unusually large size of the pCaSpeRIV transformation vector. Various difficulties surfaced early on. The first was a problem with the phosphatase. Calf Intestinal Alkaline Phosphatase (CIP) was used to remove the phosphate groups from the 5' end of pCaSpeRIV, but when these CIP treated vectors were used for ligations, the result was always zero colony growth. The phosphatase of choice was then changed to Antarctic Phosphatase (AP). AP was used in the successful ligation of $\beta 1\beta 2C$ into pBlueScript II SK+, so there was precedent for the use of AP throughout the remainder of the study. AP was more easily inactivated than CIP, but it did not

have high fidelity in removing every 5' phosphate group. The result was that there tended to be a lot of background colony growth. That is, the transformed ligation reactions would produce many colonies that were not the result of successful ligation, but the re-closing of the vector with itself. The sheer number of colonies produced made the plasmid prep and *EcoRI* digest screening method too time consuming and costly.

The use of PCR colony screening was very useful at expediting the process of screening for successful ligations, increasing efficacy by 4 to 5 fold. Yet, even with the mass screening of hundreds of bacterial colonies from nearly two hundred ligation reactions, there was no true positive result returned.

There were, however, a couple of instances of false positive results. The first came in the form of an ambiguous result returned from PCR screening. Because this result looked promising, it was further investigated by *PstI* digestion. The *PstI* digest also showed successful ligation of pCaSpeRIV + $\beta 2\beta 1\beta 2$. This result was suspicious, though, because it indicated that ligation had occurred in 7 out of the 9 colonies that were screened. In order to triple check the samples, the *Eco0109* screening method was devised. Even the results of this method were consistent with what was expected for a positive result. This made it even more disheartening when it was found out that there was not an insert in pCaSpeRIV at all. At the heart of this mistake was the believed number of *PstI* cut sites in pCaSpeRIV. It is true that unaltered pCaSpeRIV sequence does have just a single *PstI* cut site but, as was discovered through thorough sequence analysis, the altered, $\beta 2$ regulatory sequence-containing version of pCaSpeRIV contains two *PstI* cut sites. Consequently, there were two DNA bands when a *PstI* digest was performed not because of the presence of an insert, but because there was an extra unknown *PstI* restriction site. This site was introduced by the creators of our specific version of

pCaSpeRIV vector when they modified it by adding $\beta 2$ tubulin regulatory sequence. This mistaken belief in the number of *PstI* cut sites, made a negative result appear to be a positive one.

There were some positive developments as a direct result of the fastidious ligation process. Two possible alternatives to ligation were explored with mixed, but promising, results.

The first alternative attempted was the lipofection method of gene expression. Preliminary data indicated that it was possible to express $\beta 2$ tubulin in the testes, but the limiting factor was maintaining healthy testes tissue in culture for a long enough period of time for full expression of the phenotype. If preliminary data are correct, this method merits full investigation because it may be possible express chimeric versions of $\beta 1$ - $\beta 2$ tubulin without transferring them into pCaSpeRIV from pBlueScript II SK+.

The second alternative to ligation into pCaSpeRIV was direct mutagenesis of the chimeric insert while it is in pCaSpeRIV. While initial attempts using this method were unsuccessful, it still holds the most promise of any of the possible alternatives. If a method of site-directed mutagenesis could be perfected without having to transfer the insert back and forth between pBlueScript II SK+ and pCaSpeRIV, this would significantly simplify and expedite the entire project. Many more chimeric versions of $\beta 1$ - $\beta 2$ tubulin could be tested and the functionally important differences between $\beta 1$ tubulin and $\beta 2$ tubulin could be identified with increased rapidity. Specifically, perhaps if non-mutagenic intermediary pCaSpeRIV primers were designed to act as stop gaps to fill the in-between space of the vector, the polymerase may be able to circumnavigate the full length of the vector. Again, perfection of this method would serve as an excellent alternative to the ligation method.

Conclusions

It does not appear that there is any physical explanation for the inability of the chimeric $\beta 2\beta 1\beta 2$ or $\beta 1\beta 2\beta 2$ to ligate into pCaSpeRIV. The positive control ligations demonstrated that when pBlueScript II SK+ with $\beta 2\beta 1\beta 2$ insert was *EcoRI* digested and then directly ligated back together, successful ligation was possible. The same could not be said for the positive control ligation of pCaSpeRIV + $\beta 1\beta 2C$. This result is revealing in that it appears to absolve the insert of the blame for the failed ligation reactions. However, it does not necessarily implicate the vector as being solely culpable. In any case, it is nice to know that at least one of main components is capable of ligation, but it only makes more perplexing the question of *why* the experimental ligation reaction would not work.

Based on what can be inferred from the combination of the above results, it appears that the reaction is completely possible, just not very probable. Considering the exceptional size of the pCaSpeRIV and the repeated success of ligation using the much smaller vector, pBlueScript II SK+, the whole situation may just be a problem of kinetics. The large vector makes it highly unlikely that the two sticky *EcoRI* cut ends of its DNA will occupy the same time and space as the two complimentary sticky ends of the insert in a ligation reaction. It is by no means an impossible event, however. The answer may just lie in a continued brute force effort of: ligation \rightarrow transformation \rightarrow PCR screening, until that elusive and improbable ligation event is recovered.

Chapter III.
Development of a Nanoparticle Toxicity Assay Using *Drosophila melanogaster* as a
Model Organism

Introduction

Nanomaterials are engineered structures with at least one dimension of 100 nanometers or less. These materials are increasingly being used for commercial purposes such as fillers, opacifiers, catalysts, semiconductors, cosmetics, microelectronics, and drug carriers. The market for nanotechnologies is estimated to be \$700 billion for 2008 and more than \$1 trillion by 2015 by the US National Science Foundation (NSF).

Materials in this size range may approach the length scale at which some specific physical or chemical interactions with their environment can occur. As a result, their properties differ substantially from bulk materials of the same composition, allowing them to perform exceptional feats of conductivity, reactivity, and optical sensitivity (Kamat 2002, Schwerdtfeger 2003). While nanoscale materials possess more novel and unique physicochemical properties than bulk materials, they also have an unpredictable impact on human health and the environment (Nel *et al.*, 2006).

To date, there have been a limited number of studies that have investigated the toxicological and environmental effects of direct and indirect exposure to nanomaterials and no clear guidelines exist to quantify these effects. The establishment of principles and test procedures to ensure safe manufacture and use of nanomaterials is urgently required.

Nanoparticles are presented as an aerosol (mostly solid or liquid phase in air), a suspension (mostly solid in liquids) or an emulsion (two liquid phases). Historically, most nanoparticle toxicity studies have involved ingestion or injection methods using mammalian cells or live mammals. These methods are both time and cost prohibitive. Studies of the toxicological effects of nanoparticles *via* inhalation are scarce. Determination of the potential toxic effects of inhaled nanoparticles is of particular importance due to the increased exposure of

humans to nanomaterials in the work environment and the increased emission of nanoparticles into the atmosphere. Of further concern, research has shown that some nanomaterial agents that seem harmless when administered orally or dermally are toxic to the lungs when inhaled (Fubini and Are'an, 1999). To address this, a novel model system using *Drosophila melanogaster* is being developed as a quick assay of nanoparticle toxicity.

The Model Organism

To better understand how the aerosolized nanoparticles are delivered to the tracheal system of *D. melanogaster*, it is important to understand basic fly anatomy and physiology. Insects do not breathe through their mouths as we do. They do not have lungs and their blood, which is typically a watery, yellowish liquid, does not carry oxygen and carbon dioxide through their bodies. Insects have a system of tubes, called tracheae, instead of lungs. These tracheae penetrate right through the insect's body. Air enters the tracheae by pores called spiracles. These spiracles are found on each side of the insect's abdomen and each segment of the abdomen has a pair of spiracles (Fig. 29A). The air passes into the tracheal system *via* the spiracles and into smaller and smaller tubes, in a similar way to the bronchioles in our lungs (Fig. 29B&C). The tracheae finally end in the tissues which are respiring (Mackean and Mackean, 1988).

The Method of Delivery

Drug delivery *via* inhalation has been utilized in the medical field for the treatment of asthma symptoms, pain medication, and various sinus treatments, among other things. There is also precedent for the use of aerosolizing devices in *D. melanogaster*. Broderick *et al.* used a commercial nebulizer to deliver cobalamin to *D. melanogaster* as a successful cyanide antitoxin

(Broderick *et al.* 2000). This same concept is applied to deliver various nanomaterials to *D. melanogaster* via inhalation of the particles into their tracheal system.

Methods

In order to prove that the method works as described, it first must be shown that the nanoparticles are aerosolized by the nebulizer and, secondly, that these aerosolized particles enter the tracheal system of the flies.

The first step was clearly demonstrated using three different particles: 24 nm green fluorescent polystyrene Fluospheres (Invitrogen), 10 nm silver particles, and 5-6 nm CdSe/ZnS quantum dots.

Fluospheres

In order to replicate the exact conditions of the future fly experiments, the mouthpiece of a nebulizer (Minimate compressor, model #PM5, Precision Medical, INC. Northampton, PA) was attached to a 1 x 3 cm chamber consisting of plastic tubing with cotton meshing at the proximal and distal ends of the of the chamber to reduce rate of air flow, minimize turbulence, and prevent escape of the flies (Fig. 30). Hole punch sized pieces of filter paper were placed into the chamber and exposed to nebulized 24 nm green fluorescent (50 $\mu\text{g/mL}$) Fluospheres for 5 minutes. After exposure, the filter paper was examined for fluorescence under a fluorescent microscope.

Silver Nanoparticles

The same method described for the Fluospheres was used for nebulization of 10 nm silver particles (50 $\mu\text{g/mL}$). Also, in place of the filter paper, carbon mesh grids were used. After exposure, the carbon grids were examined using a transmission electron microscope (TEM).

CdSe/ZnS quantum dots

Once again, the same procedure described for the Fluosperes was used for nebulization of 5-6 nm CdSe/ZnS quantum dots (50 µg/mL). In place of the pieces of filter paper, wild-type Oregon RS *Drosophila melanogaster* from the Bloomington Stock Center (Bloomington, IN), and reared on Bloomington Stock Center Standard Cornmeal Media at 25°C, were used. Virgin adult flies were anesthetized using CO₂ gas, placed into the 1 x 3 cm chamber and allowed to equilibrate to the chamber for 10 minutes. The flies were exposed to nebulized CdSe/ZnS quantum dots for 5 minutes and then frozen at -70°C. At a later date, the flies were examined for fluorescence under a fluorescent microscope.

Results

Fluospheres

The Fluospheres were successfully aerosolized by the nebulizer. All of the green fluorescence seen can be attributed to the fluorescence of the Fluospheres (Fig. 31). Negative control (not shown) pieces of filter paper showed no green fluorescence.

Silver Nanoparticles

The silver nanoparticles were capable of being aerosolized by the nebulizer (Fig. 32). They did not appear to be as uniformly distributed as the Fluospheres. This may have been due to the unexpected large variation (5-160nm) of the particles in combination with their strong tendency to agglomerate. This is consistent with indications from additional Fluosphere research that excessively large particles, >180 nm, do not nebulize at a comparable rate to smaller, < 180 nm, particles.

CdSe/ZnS

The CdSe/ZnS particles were also successfully aerosolized (Fig. 33). This is evident by the brightly fluorescent red color coating the experimental fly. Under identical fluorescence conditions, the unexposed negative control fly shows little to no red fluorescence. This is the method that will be utilized to demonstrate the second premise of the inhalation method; proof that nanoparticles enter the tracheal system.

Discussion

It was necessary to show that the nebulizer was capable of aerosolizing all three of the particles. This was important because each of the particles was physically much different from the other two.

The Fluospheres are basically plastic and nebulization of them alone would not necessarily infer that the much more dense metal particles would give the same result. Their main usefulness was in their easy visualization due to their fluorescent properties. The silver nanoparticles are more relevant to the types of studies that this method is designed to perform, however, it is much more difficult to visualize because it does not fluoresce. Nonetheless, silver nanomaterial is a common product in the manufacturing industry and also serves an analogous type of particle to many of the other materials that we hope to test. As we found to be the case with many of the other metal nanomaterials that we purchased, the so called 10 nm silver particles were on average closer to ~100 nm in size. The cause of this was two fold: 1. there was little quality control in the manufacturing of the particles and the result was a range of particles from 5-160nm, 2. due to surface charge interactions, metal particles tend to agglomerate when suspended in water. Although these were not desirable qualities for working with the silver particles, the “silver” lining was that the nebulizer demonstrated that it was capable of aerosolizing metal particles of up to at least 160 nm in size.

CdSe/ZnS has the most potential in helping to prove the inhalation method using the nebulizer. It is both a stable, non-agglomerating metal and has strong fluorescent properties. As can be seen in Fig. 36, the particles can easily be distinguished on the exposed flies. If the second part of the inhalation method in flies (actually showing that the nanoparticles enter the

flies tracheal system) is to be proven, it most likely going to occur through the use of these particles.

Now that design of the experiment has been finalized and all preliminary results, so far, seem to indicate that the system is functional, the next steps will be: to verify that the nanoparticles enter the tracheal system of the fly, determine if the nanoparticles cross the epithelium of the tracheal wall, test the effects on survivorship of nanoparticles other than silver, and begin assays of nanoparticle effects at the cellular level.

Conclusions

As the use of nanomaterials continues to grow at an exponential rate, and with constant development of new versions of nanoparticles, a quick and effective method of toxicological analysis is becoming more and more of a necessity. Due to the time and cost constraints of current nanoparticles toxicity assays, there threatens to be a growing lag time between nanoparticle development and nanoparticle toxicity assessment. Considering the minimal cost and potentially high yield of information, the quick assay method proposed above has the potential to fill this rapidly widening gap.

REFERENCES

1. Aktipis, S., and Panayotatos, N. 1976. Mechanism of ethidium bromide inhibition of RNA polymerase. *Biochem. Biophys. Res. Commun.* 68 (2): 465–470.
2. Alberts, B., Bray, D., Lewis, J., Raff, M., Roberts, K., and Watson, J. 1983. *Molecular Biology of the Cell*. New York: Garland.
3. Brittle AL, Ohkura H. Mini spindles, the XMAP215 homologue, suppresses pausing of interphase microtubules in *Drosophila*. *Embo J* 2005 ;24:1387–1396.
4. Broderick, K.E., Potluri, P., Zhuang, S., Scheffler, I.E., Sharma, V.S., Pilz, R.B., Boss, G.R. 2006. Cyanide detoxification by the cobalamin precursor cobinamide. *Exp Biol Med.* 231: 641–649.
5. Burbank, K.S., and Mitchison, T.J. 2006. Microtubule dynamic instability. *Current Biology.* 16 (14): R516-R517.
6. Chang, P., Giddings T.H. Jr, Winey, M., Stearns, T. 2003. Epsilon-tubulin is required for centriole duplication and microtubule organization. *Nat. Cell. Biol.* 5: 71-76.
7. Dallai, R., and Afzelius, B.A. 1990. Microtubular diversity in insect spermatozoa: results obtained with a new fixative. *Journal of Structural Biology.* 103 (2): 164-179.
8. Dallai, R., and Afzelius, B.A. 1993. Development of the accessory tubules of insect sperm flagella. *Journal of Submicroscopic Cytology and Pathology.* 25 (4): 499-504.
9. Dallai, R., Lupetti, P., and Mencarelli, C. 2006. Unusual axonemes of hexapod spermatozoa. *International Review of Cytology: A Survey of Cell Biology.* 254: 45-99.
10. Dorus, S., Busby, S.A., Gerike, U., Shabanowitz, J., Hunt, D.F., and Karr, T.L. 2006. Genomic and functional evolution of the *Drosophila melanogaster* sperm proteome. *Nature Genetics.* 38: 1440-1445.
11. Dutcher, S.K. 1995. Flagellar assembly in two hundred and fifty easy-to-follow steps. *Trends in Genetics.* 11 (10): 398-404.
12. Dutcher, S.K. 2003. Long-lost relatives reappear: identification of new members of the tubulin superfamily. *Current Opinion in Microbiology.* 6: 634–640
13. Fubini, B., and Otero Areán, C. 1999. Chemical aspects of the toxicity of inhaled mineral dusts. *Chem. Soc. Rev.* 28: 373-381.
14. Fuller, M. 1993. Spermatogenesis. In: Bate, M., and Martinez Arias, A., editors. *The Development of Drosophila melanogaster*, 2nd ed. Cold Spring Harbor (NY): Cold Spring Harbor Laboratory. p. 71-147.
15. Gibbons, I.R. 1981. Cilia and flagella of eukaryotes. *J. Cell. Biol.* 91 (3): 107-124.
16. Graur, D., and Li, W.H. 2000. *Fundamentals of Molecular Evolution*. Sunderland (MA): Sinauer Associates. p. 104.
17. Han, Y.G., Kwok, B.H., and Kernan, M.J. 2003. Intraflagellar transport is required in *Drosophila* to differentiate sensory cilia but not sperm. *Current Biology.* 13 (19): 1679-1686.
18. Hoyle, H.D., and Raff, E.C. 1990. Two *Drosophila* beta tubulin isoforms are not functionally equivalent. *J. Cell. Biol.* 111 (3): 1009-1026.
19. Inoue, H., Nojima, H., and Okayama, H. (1990) High efficiency transformation of *Escherichia coli* with plasmids. *Gene.* 96: 23-28.

20. Kaltschmidt, B., Glätzer, K.H., Michiels, F., Leiss, D., and Renkawitz-Pohl, R. 1991. During *Drosophila* spermatogenesis $\beta 1$, $\beta 2$, and $\beta 3$ tubulin isotypes are cell-type specifically expressed but have the potential to coassemble into the axoneme of transgenic flies. *Eur. J. Cell. Biol.* 54: 110-120.
21. Kamat, P.V. 2002. Photophysical, photochemical and photocatalytic aspects of metal nanoparticles. *J. Phys. Chem. B.* 106 (32): 7729-7744.
22. Kemphues, K.J., Kaufman, T.C., Raff, R.A., Raff, E.C. 1982. The testis-specific β -tubulin subunit in *Drosophila melanogaster* has multiple functions in spermatogenesis. *Cell.* 31: 655-670.
23. Kerssemakers JW, Munteanu EL, Laan L, Noetzel TL, Janson ME, Dogterom M. Assembly dynamics of microtubules at molecular resolution. *Nature* 2006; 442:709-712.
24. Kidwell, M.G. 1983. Evolution of hybrid dysgenesis determinants in *Drosophila melanogaster*. *Proc. Nat. Acad. Sci. USA.* 80 (6): 1655-1659.
25. Kinoshita K, Arnal I, Desai A, Drechsel DN, Hyman AA. Reconstitution of physiological microtubule dynamics using purified components. *Science* 2001; 294:1340-1343.
26. Kozminski, K.G., Johnson, K.A., Forscher, P., and Rosenbaum, J.L. 1993. A motility in the eukaryotic flagellum unrelated to flagellar beating. *Proc. Nat. Acad. Sci. USA.* 90 (12): 5519-5523.
27. Lehmann, F.-O., and Heymann, N. 2005. Unconventional mechanisms control cyclic respiratory gas release in flying *Drosophila*. *J. Exp. Biol.* 208: 3645-3654.
28. Löwe, J., Li, H., Downing, K.H., and Nogales, E. 2001. Refined structure of $\alpha\beta$ -tubulin at 3.5 Å resolution. *J. Mol. Biol.* 313 (5): 1045-1057.
29. McNally, F. J. 1999. Microtubule dynamics: Controlling split ends. *Current Biology.* 9(8): R274-R276.
30. Michiels, F., Falkenburg, D., Müller, A.M., Hinz, U., Otto, U., and Bellman, R. 1987. Testis-specific $\beta 2$ tubulins are identical in *Drosophila melanogaster* and *D. hydei* but differ from ubiquitous $\beta 1$ tubulin. *Chromosoma.* 95 (6): 387-395.
31. Mitchison, T., and Kirschner, M. 1984. Dynamic instability of microtubule growth. *Nature.* 312: 237-242.
32. Miyaki, M., Ono, T., and Umezawa, H. 1971. Inhibition of ligase reaction by bleomycin. *J. Antibiotics.* 24: 587-592.
33. Moores CA, Milligan RA. Lucky 13-microtubule depolymerisation by kinesin-13 motors. *J Cell Sci* 2006; 119:3905-3913.
34. Morrow, E. H. 2004. How the sperm lost its tail: the evolution of aflagellate sperm. *Biological Reviews.* 79: 795-814.
35. Nel, A., Xia, T., Mädler, L., and Li, N. 2006. Toxic potential of materials at the nanolevel. *Science.* 311 (5761): 622-627.
36. Nielsen MG, Raff EC. 2002. The best of all worlds or the best possible world? Developmental constraint in the evolution of beta tubulin and the sperm tail axoneme. *Evol. Dev.* 4(4): 303-315.
37. Nielsen, M.G., Caserta, J.M., Kidd, S.J., and Phillips, C.M. 2006. Functional constraint underlies 60 million year stasis of Dipteran testis-specific β -tubulin. *Evolution & Development.* 8 (1): 23-29.
38. Nielsen, M.G., Turner, F.R., Hutchens, J.A., and Raff, E.C. 2001. Axoneme-specific β -tubulin specialization: a conserved C-terminal motif specifies the central pair. *Current Biology.* 11 (7): 529-533.

39. Nogales, E., and Wang, H.-W. 2006. Structural intermediates in microtubule assembly and disassembly: how and why? *Current Opinion in Cell Biology*. 18 (2): 179-184.
40. Nogales, E., Whittaker, M., Milligan, R.A., and Downing, K.H. 1999. High-resolution model of the microtubule. *Cell*. 96 (1): 79-88.
41. Nogales, E., Wolf, S.G., and Downing, K.H. 1998. Structure of the alpha beta tubulin dimer by electron crystallography. *Nature*. 391 (6663): 199-203.
42. Nonaka, S., Tanaka, Y., Okada, Y., Takeda, S., Harada, A., Kanai, Y., Kido, M., and Hirokawa, N. 1998. Randomization of left-right asymmetry due to loss of nodal cilia generating leftward flow of extraembryonic fluid in mice lacking KIF3B motor protein. *Cell*. 95: 829-837.
43. Omoto, C.K., Gibbons, I.R., Kamiya, R., Shingyoji, C., Takahashi, K., and Witman, G.B. 1999. Rotation of the central pair microtubules in eukaryotic flagella. *Mol. Biol. Cell*. 10 (1): 1-4.
44. Pitnick, S., Spicer, G.S., and Markow, T.A. 1995. How long is a giant sperm? *Nature*. 375: 109.
45. Popodi, E.M., Hoyle, H.D., Turner, F.R., Xu, K., Kruse, S., and Raff, E.C. 2008. Axoneme specialization embedded in a "Generalist" beta-tubulin. *Cell. Motil. Cytoskeleton*. 65: 216-237.
46. Porter, M., Bower, K., Knott, J., Byrd, P., and Dentler, W. 1999. Cytoplasmic dynein heavy chain 1b is required for flagellar assembly in *Chlamydomonas*. *Mol. Biol. Cell*. 10 (3): 693-712.
47. Quicke, D.L.J., Ingram, S.N., Baillie, H.S., and Gaitens, P.V. 1992. Sperm structure and ultrastructure in the Hymenoptera (Insecta). *Zoologica Scripta*. 21 (4): 381-402.
48. Raff, E.C. 1994. The role of multiple tubulin isoforms in cellular microtubule function. In: Hyams, J.S., and Lloyd, C.W., editors. *Microtubules*. New York: John Wiley & Sons. p. 85-110.
49. Raff, E.C., Fackenthal, J.D., Hutchens, J.A., Hoyle, H.D., and Turner, F.R. 1997. Microtubule architecture specified by a β -tubulin isoform. *Science*. 275 (5296): 70-73.
50. Raff, E.C., Hutchens, J.A., Hoyle, H.D., Nielsen, M.G., and Turner, F.R. 2000. Conserved axoneme symmetry altered by a component β -tubulin. *Current Biology*. 10 (21): 1391-1394.
51. Roberts, K. and Hyams, J., editors. 1977. *Microtubules*. London: Academic.
52. Rogers SL, Rogers GC, Sharp DJ, Vale RD. Drosophila EB1 is important for proper assembly, dynamics, and positioning of the mitotic spindle. *J Cell Biol* 2002;158:873-884.
53. Rosenbaum, J. 2000. Cytoskeleton: Functions for tubulin modifications at last. *Current Biology*. 10 (21): R801-R803.
54. Rubin, G.M., Yandell, M.D., Wortman, J.R., Gabor Miklos, G.L., Nelson, C.R., Hariharan, I.K., Fortini, M.E., Li, P.W., Apweiler, R., Fleischmann, W., Cherry, J.M., Henikoff, S., Skupski, M.P., Misra, S., Ashburner, M., Birney, E., Boguski, M.S., Brody, T., Brokstein, P., Celniker, S.E., Chervitz, S.A., Coates, D., Cravchik, A., Gabrielian, A., Galle, R.F., Gelbart, W.M., George, R.A., Goldstein, L.S., Gong, F., Guan, P., Harris, N.L., Hay, B.A., Hoskins, R.A., Li, J., Li, Z., Hynes, R.O., Jones, S.J., Kuehl, P.M., Lemaitre, B., Littleton, J.T., Morrison, D.K., Mungall, C., O'Farrell, P.H., Pickeral, O.K., Shue, C., Vossball, L.B., Zhang, J., Zhao, Q., Zheng, X.H., Lewis, S. 2000. Comparative genomics of the eukaryotes. *Science*. 287 (5461): 2204-2215.

55. Rudolph, J.E., Kimble, M., Hoyle, H.D., Subler, M.A., and Raff, E.C. 1987. Three *Drosophila* β -tubulin sequences: a developmentally regulated isoform ($\beta 3$), the testis-specific isoform ($\beta 2t$ 8) reveal both an ancient divergence in metazoan isotypes and structural constraints for β -tubulin function. *Mol. Cell. Biol.* 7 (6): 2231-2242.
56. Samsonov A, Yu JZ, Rasenick M, Popov SV. Tau interaction with microtubules *in vivo*. *J Cell Sci* 2004; 117:6129–6141.
57. Schwerdtfeger, P. 2003. Gold goes nano—From small clusters to low-dimensional assemblies. *Angewandte Chemie, Int. Ed.* 42 (17): 1892-1895.
58. Signor, D., Wedaman, K.P., Orozco, J.T., Dwyer, N.D., Bargmann, C.I., Rose, L.S., and Scholey, J.M. 1999. Role of a class DHC1b dynein in retrograde transport of IFT motors and IFT raft particles along cilia, but not dendrites, in chemosensory neurons of living *Caenorhabditis elegans*. *J. Cell. Biol.* 147 (3):519-530.
59. Takeda, S., Yonekawa, Y., Tanaka, Y., Okada, Y., Nonaka, S., and Hirokawa, N. 1999. Left-right asymmetry and kinesin superfamily protein KIF3A: new in-sights in determination of laterality and mesoderm induction by *kif3A*^{-/-} mice analysis. *J. Cell. Biol.* 145 (4): 825-836.
60. Turner, R.M. 2003. Tales from the tail: what do we really know about sperm motility? *Journal of Andrology.* 24 (6): 790-803.
61. Warner, F.D. 1972. Macromolecular organization of eukaryotic cilia and flagella. In: *Advances in Cell and Molecular Biology*. DuPraw, E.J., editor. 2: 192-235.
62. Warner, F.D., and Satir, P. 1974. The structural basis of ciliary bend formation: radial spoke positional changes accompanying microtubule sliding. *J. Cell. Biol.* 63: 35-63.
63. Watt, W.B. 1985. Bioenergetics and evolutionary genetics: opportunities for new synthesis. *Am. Nat.* 125: 188-143.
64. Yamazaki, H., Nakata, T., Okada, Y., and Hirokawa, N. 1996. Cloning and characterization of KAP3: a novel kinesin superfamily-associated protein of KIF3A/3B. *Proc. Nat. Acad. Sci. USA.* 93: 8443-8448.

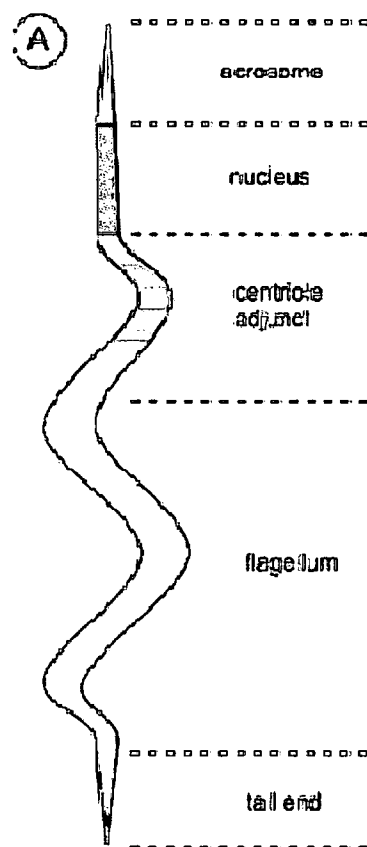


Figure 1. Schematic representation of the ground plan of a pterygote insect flagellosperm and its ultrastructure. (Turner, 2003).

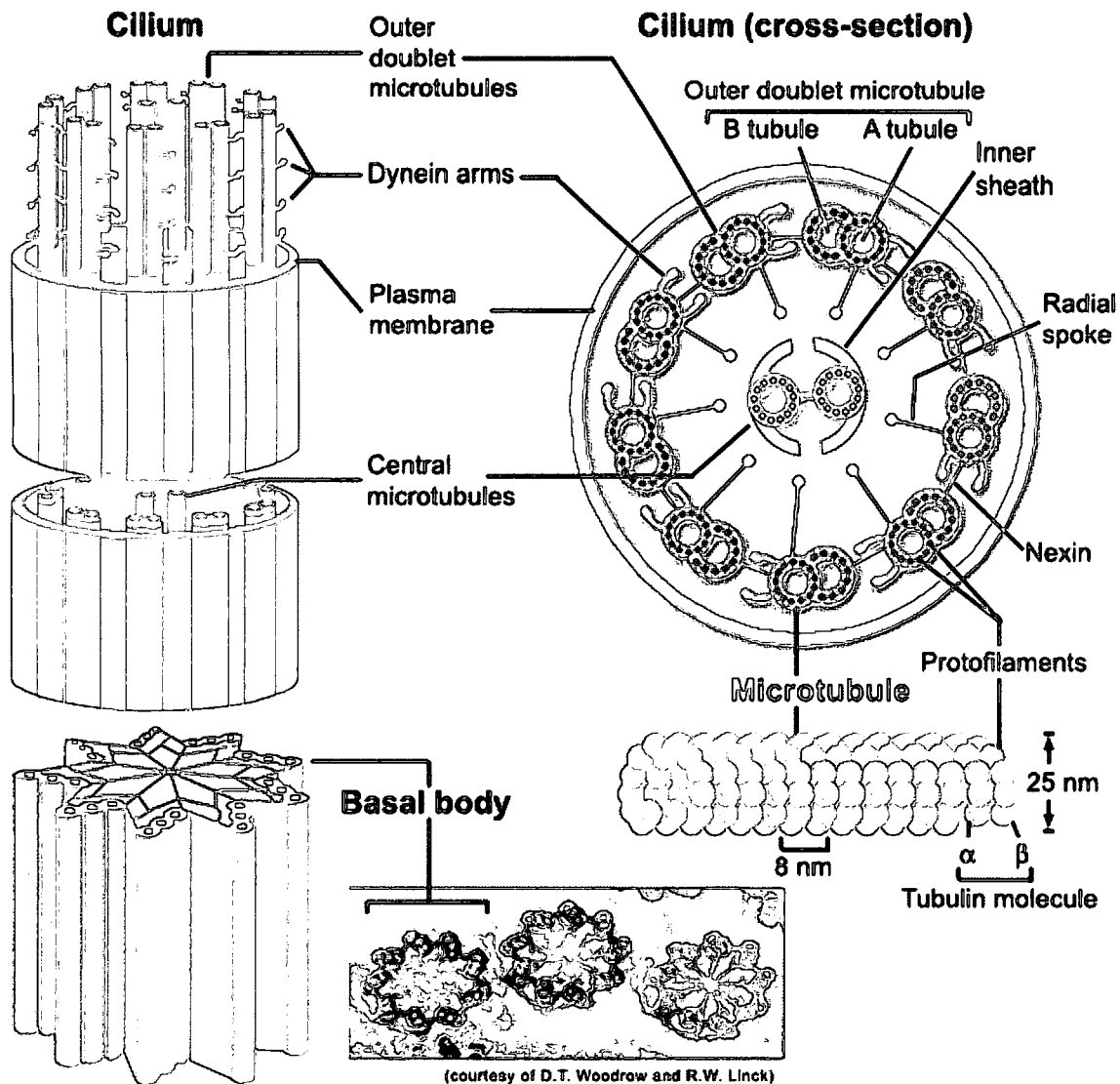


Figure 2. Illustration of the axoneme with accessory structures. It contains the canonical 9+2 ultrastructure of nine doublet microtubules surrounding a central pair of singlet microtubules. It also has accessory tubules, inner and outer dynein arms and radial spokes. The dynein arms bind and release the adjacent doublet in an ATP-dependant manner to cause flagellar beating, while the radial spokes help regulate distal sliding in conjunction with the central pair. (Woodrow and Linck).

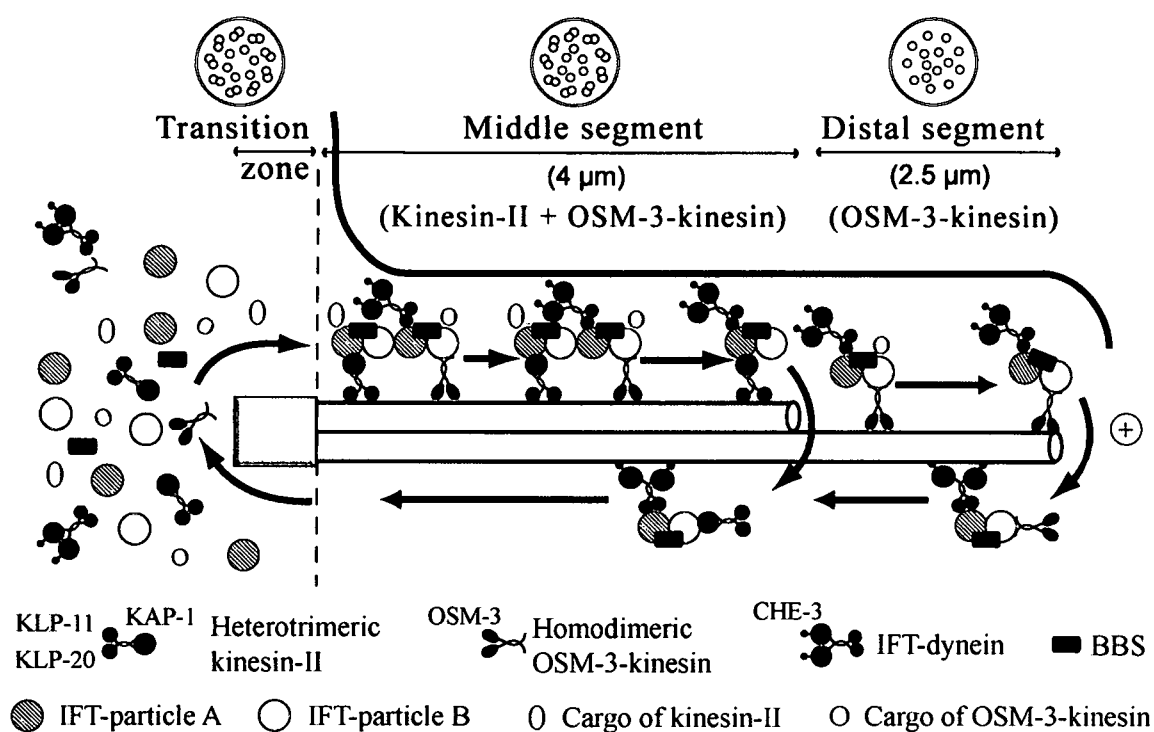


Figure 3. Intraflagellar Transport. Kinesin II is responsible for anterograde IFT towards the plus end of the microtubule, while cytoplasmic dynein controls retrograde IFT. The motor heads get their power from the hydrolysis of ATP to ADP + P_i. (Ingles et al. 1999).

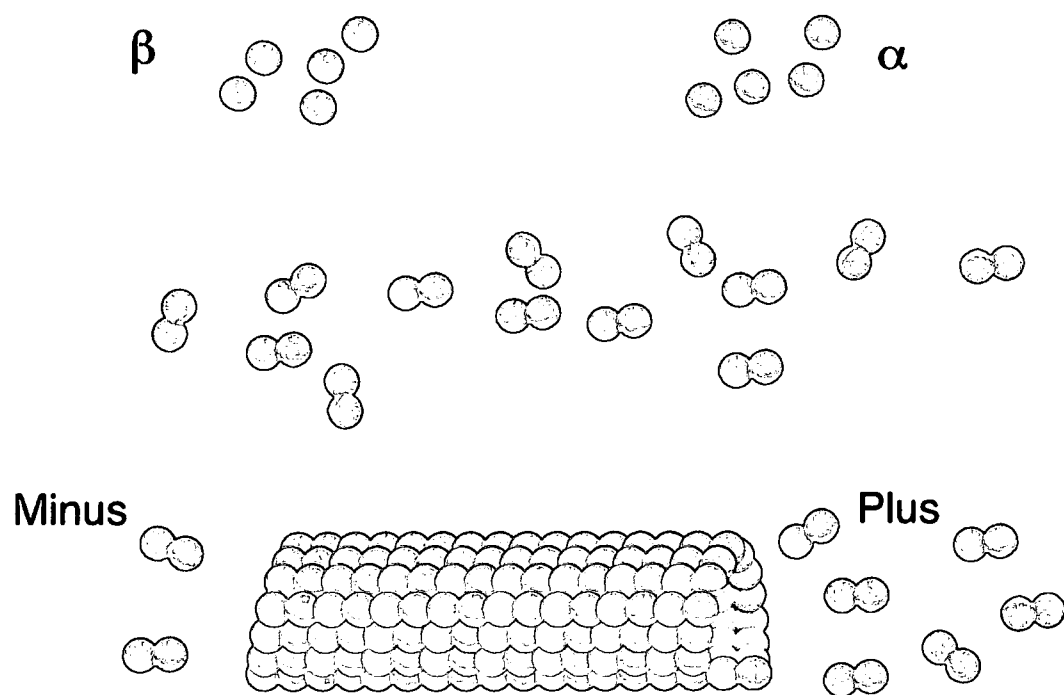


Figure 4. α and β monomers and heterodimers combine to form protofilaments. Thirteen protofilaments associate laterally to form the microtubule.

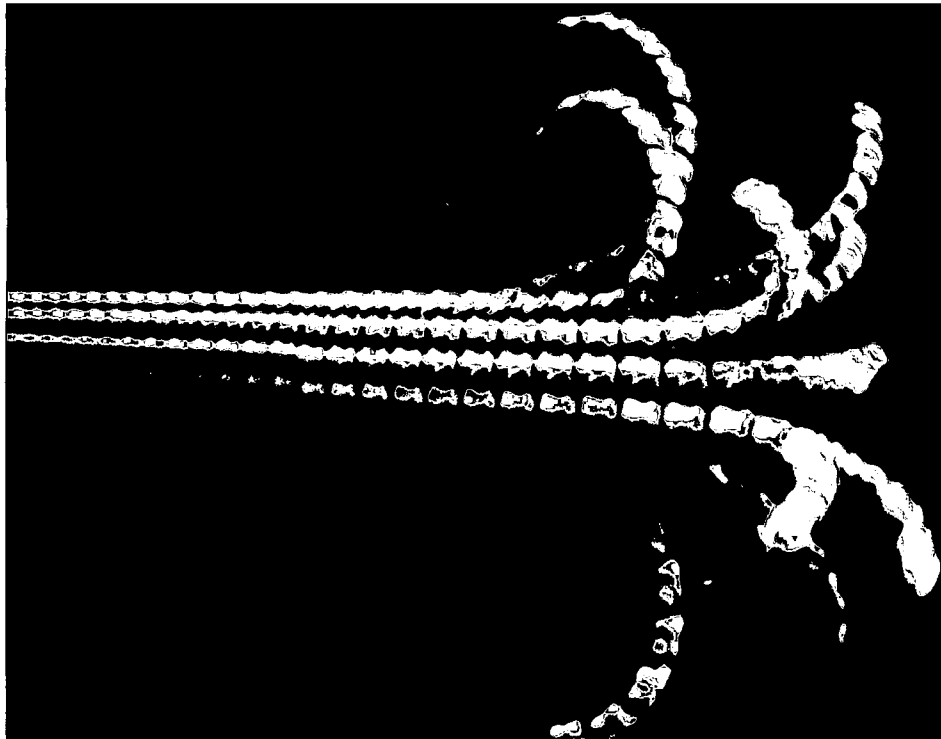


Figure 5. Dynamic instability. Hydrolysis occurs faster than the addition of the tubulin dimers. This results in the loss of the GTP cap and the microtubule becomes unstable. The protofilaments peel away and the GDP-bound tubulin returns to the cytosol to exchange its GDP for GTP. It is ready to be added to another growing microtubule. (Nogales, 2005).

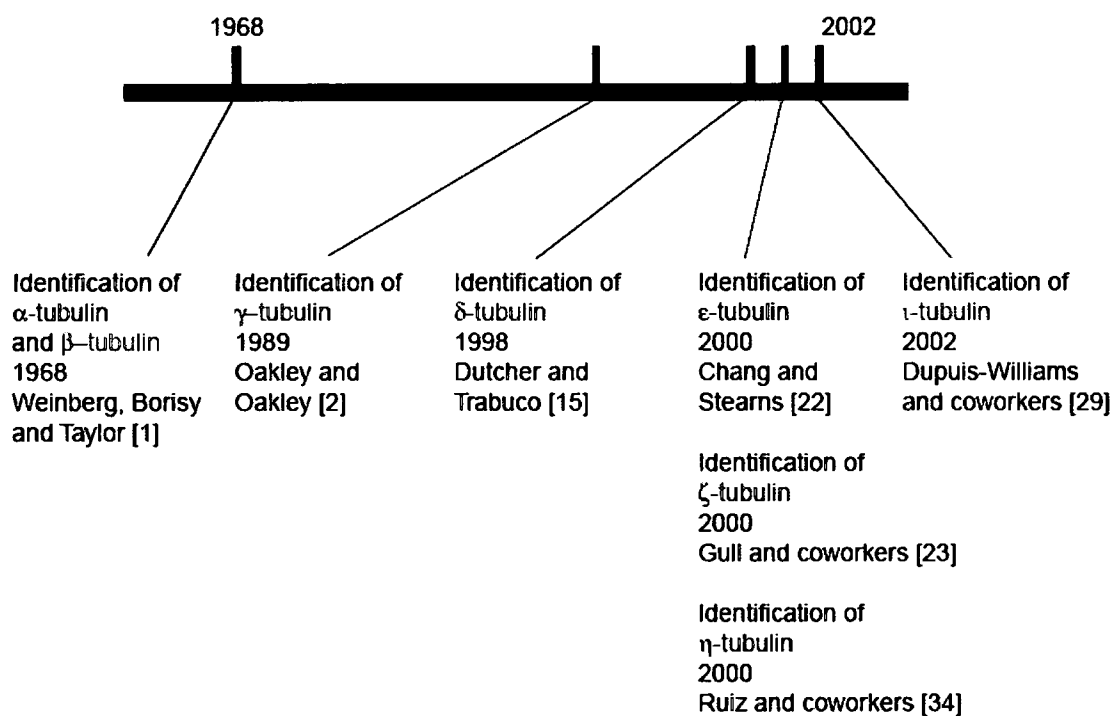


Figure 6. Timeline of the identification of members of the tubulin superfamily.

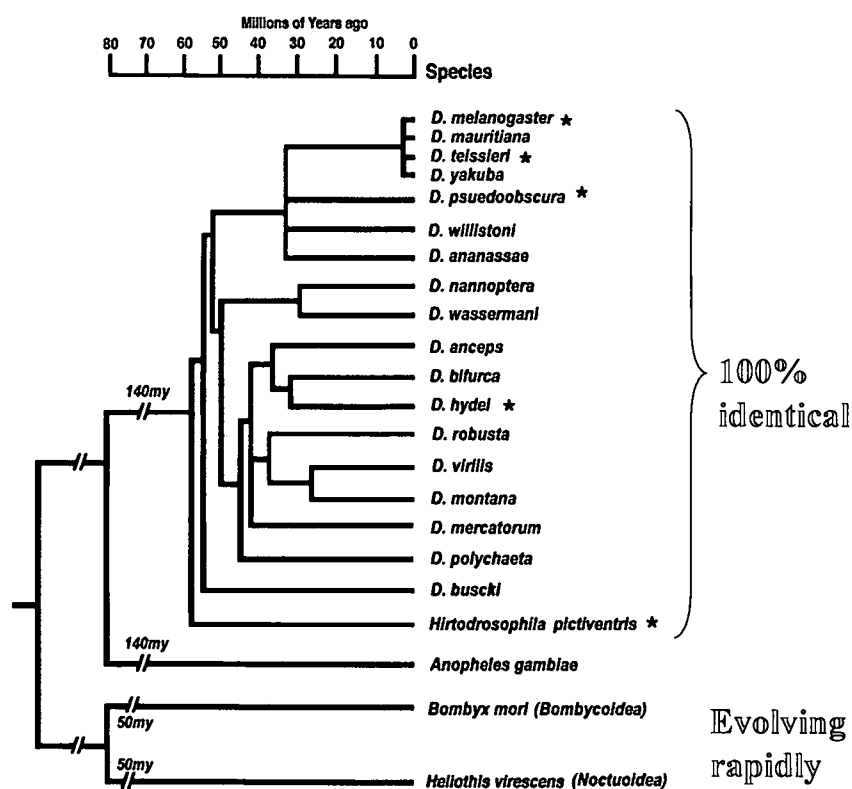


Figure 7. Phylogeny of all of the Dipteran and Lepidopteran species for which $\beta 2$ -tubulin has been sequenced. The Dipteran phylogeny represents over 60 million years of evolutionary time. (Nielsen et al. 2006).

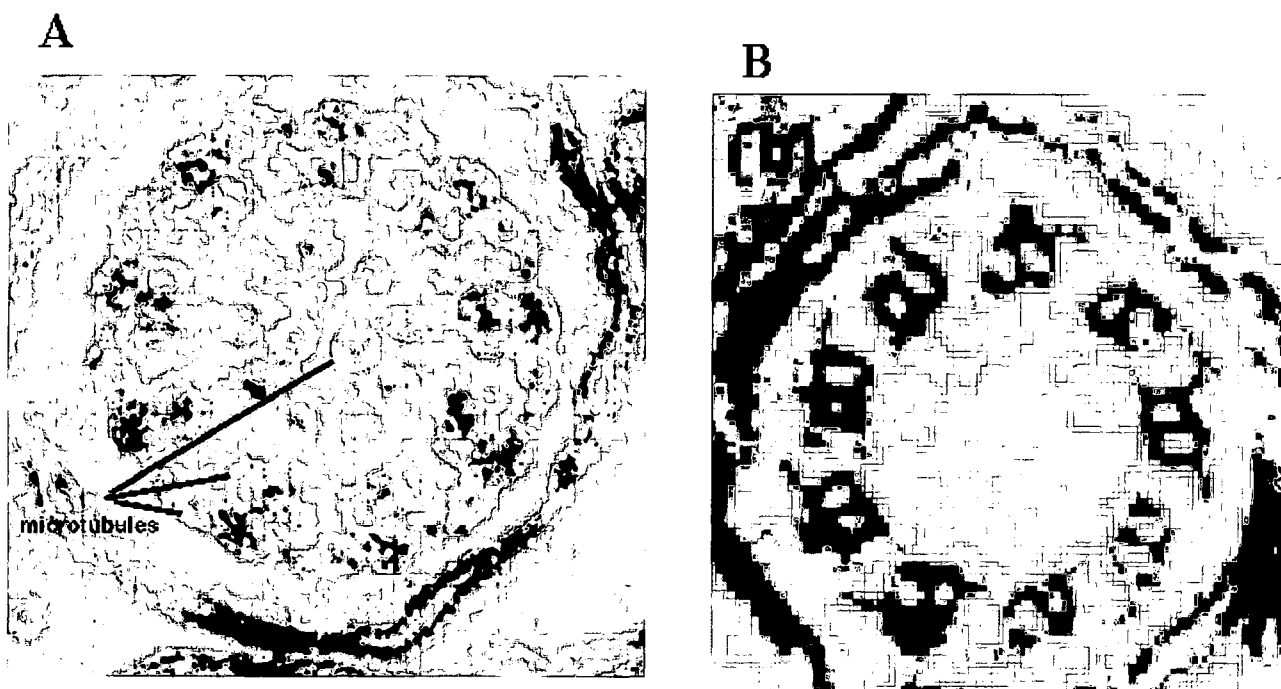


Figure 8. (A) Electron micrograph of an axoneme from a fertile male with two copies of wild-type copies of $\beta 2$. The central pair microtubules are present and morphology is normal. (B) Electron micrograph of an axoneme from a sterile male with two copies of $\beta 1$ in place of $\beta 2$. The central pair microtubules are missing but the morphology is otherwise normal. (Nielsen et al. 2001).

Beta 1 X Beta 2 Tubulin

	Nucleotide Binding Domain	Drug Binding Domain	Carboxyl Terminus
beta1	MREIVHIQAGQCGNQIGAKFWEIISDEHGIDATGTTYHGDSDLQLERINVYYNEASGGKYV		
beta2	MREIVHIQAGQCGNQIGGKFEVISDEHCIDATGTTYGDSDLQLERINVYYNEATGAKYV		
beta1	PRAVLVDLEPGTMDSVRSRPFQGIFRPDNFVFGQSGAGNNWAKGHYTEGAELVDSVLDVV		
beta2	PRAILVDLEPGTMDSVRSRFGQIFRPDNFVFGQSGAGNNWAKGHYTEGAELVDSVLDVV		
beta1	RKEAESCDCLQGFQLTHSLGGGTGSGMGTLLISKIREEYPDRSMNTYSVVPSPKVS DTVV		
beta2	RKESEGCDCLQGFQLTHSLGGGTGSGMGTLLISKIREEYPDRIMNTFSVVPSPKVS DTVV		
beta1	EPYNATLSVHQLVENTDETYCIDNEALYDICFRTLKLTTPTYGDLNHLVSLTMSGVTTCL		
beta2	EPYNATLSVHQLVENTDETYCIDNEALYDICFRTLKLTTPTYGDLNHLVSLTMSGVTTCL		
beta1	RFPGQLNADLRKLAVNMVFPRLHFFMPGFAPLTSRGSQQYRALTVPELTQQMFDAKNMM		
beta2	RFPGQLNADLRKLAVNMVFPRLHFFMPGFAPLTSRGSQQYRALTVPELTQQMFDAKNMM		
beta1	AACDPRHGRYLTVAEIFRGRMSMKEVDEQMLNIQKNSSYFVEWIPNNVKTAVCDIPPRG		
beta2	AACDPRHGRYLTVAEIFRGRMSMKEVDEQMLNIQKNSSFVEWIPNNCKTAVCDIPPRG		
beta1	LKMSATFIGNSTAIQELFKRISEQFTAMFRRKAF LHWTGEGMDEMEFTEAESNMNDLVS		
beta2	LKMSATFIGNSTAIQELFKRVSEQFTAMFRRKAF LHWTGEGMDEMEFTEAESNMNDLVS		
beta1	EYQQYQEATADEDAEFEEQEAEVDEN		
beta2	EYQQYQEATADEEGEFDEDEEGGGDE-		

Figure 9. $\beta 1$ vs. $\beta 2$ amino acid sequences, highlighting the 3 functional domains and the 25 amino acid differences between them.

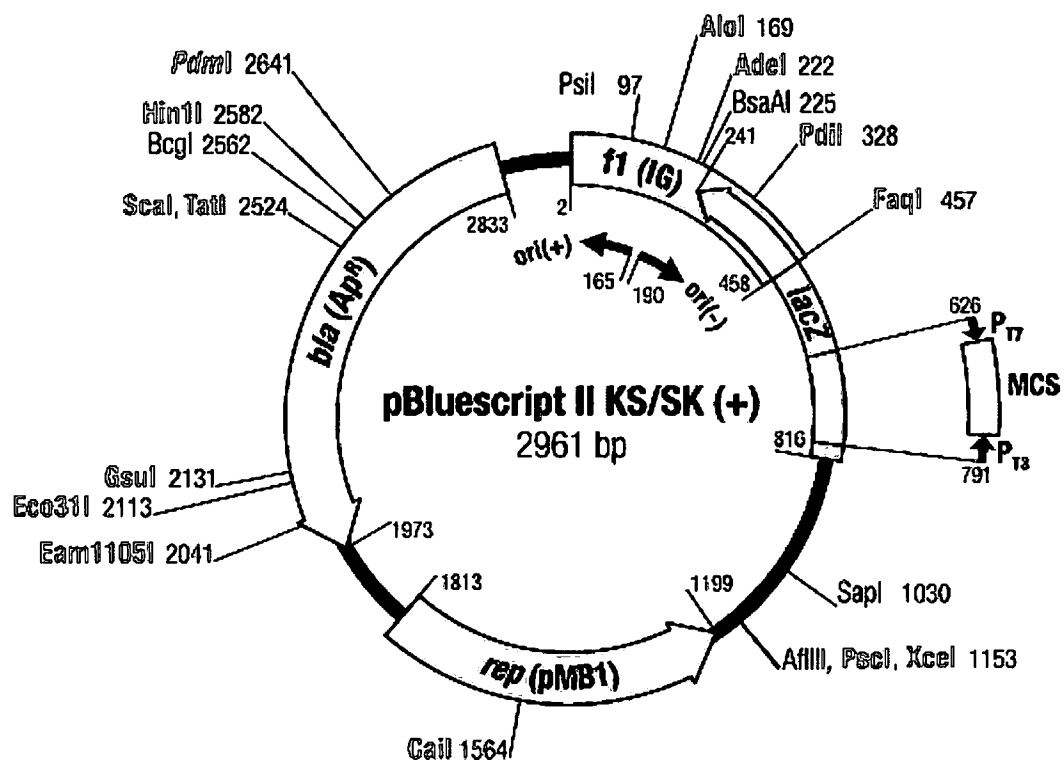


Figure 10. pBluescript II KS/SK (+) vector into which $\beta 1\beta 2C$ sequence was inserted. It is a 2961 base pair vector containing an *E. coli* and f1 helper phage origin of replication (ORI) gene, an ampicillin antibiotic resistance sequence, and a multiple cloning site (MCS) with a single *EcoRI* restriction cut site into which $\beta 1\beta 2C$ tubulin gene was inserted. Mutagenesis of $\beta 1\beta 2C$ sequence to $\beta 2\beta 1\beta 2$ and $\beta 1\beta 2\beta 2$ versions was performed in pBluescript II KS/SK (+) because of its relatively small size.

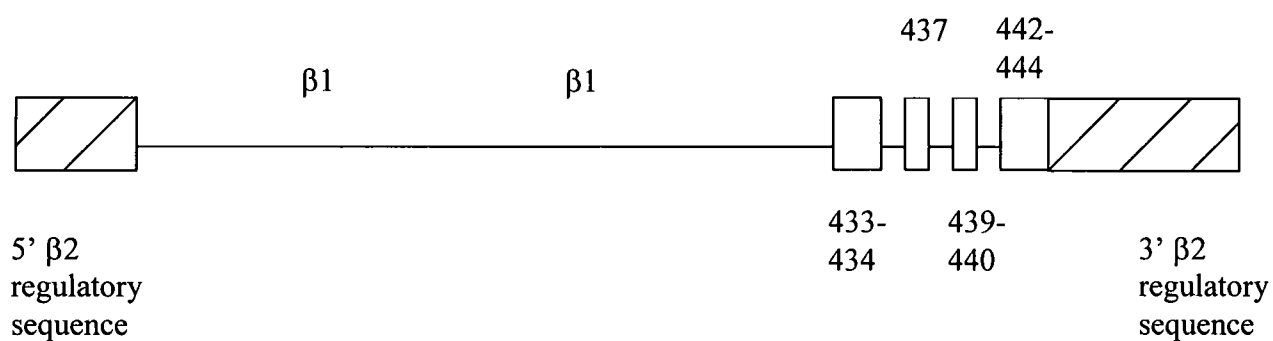


Figure 11. Template $\beta 1$ - $\beta 2$ tubulin chimeric gene, $\beta 1\beta 2C$. The striped boxes indicate the $\beta 2$ regulatory sequence. The line indicates the $\beta 1$ sequence and the red filled boxes are $\beta 2$ identity at the specified codons.

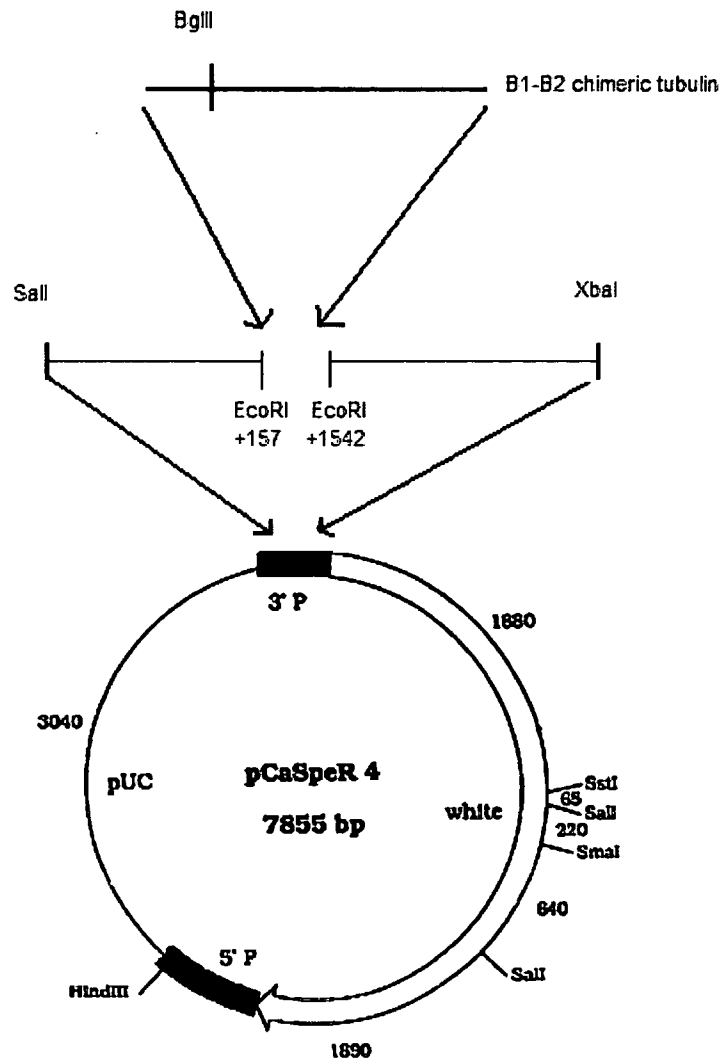


Figure 12. pCaSpeR IV vector used to insert the $\beta 1$ - $\beta 2$ chimeric gene into the *Drosophila* germline. It is a 7855 base pair P-element vector containing both the 5' and 3' P-elements necessary to integrate the chimeric gene into the *D. melanogaster* genome. It contains a copy of the white gene that is used as a phenotypic marker to track the expression of the gene, as well as, 5' and 3' $\beta 2$ tubulin regulatory sequences to ensure that the chimeric gene is expressed *in vivo* exactly like the endogenous $\beta 2$.

$\beta 1$ X $\beta 2$ Tubulin

$\beta 1$	MREIVHIQAGQCGNQIGAKFWEIISDEHGIDATGTYHGDSDLQLERINVYYNEASGGKYV
$\beta 2$	MREIVHIQAGQCGNQIGGKFWVISDEHCIDATGTYYGSDLQLERINVYYNEATGAKYV
$\beta 1$	PRAVLVDLEPGTMDSVRSGPFGQIFRPDNFVFGQSGAGNNWAKGHYTEGAELVDSVLDVV
$\beta 2$	PRAILVDLEPGTMDSVRSGRFGQIFRPDNFVFGQSGAGNNWAKGHYTEGAELVDSVLDVV
$\beta 1$	RKEAESCDCQLQGFQLTHSLGGGTGSGMGTLISKIREEYPDRSMNTYSVVPSPKVSDTVV
$\beta 2$	RKESEGCDCLQGFQLTHSLGGGTGSGMGTLISKIREEYPDRIMNTFSVVPSPKVSDTVV
$\beta 1$	EPYNATLSVHQLVENTDETYCIDNEA
$\beta 2$	EPYNATLSVHQLVENTDETYCIDNEA

Figure 13. Comparison of the nucleotide binding domain, amino acids 1-205, sequence of $\beta 1$ and $\beta 2$ tubulin. Out of the 205 amino acids of the domain, there are 12 amino acid differences.

β1 X β2 Tubulin

β1	LYDICFRTLKLTTPTYGDLNHLVSLTMSGVTTCLRFPGQLNADLRKLAVNMVFPRLHFFMPG
β2	LYDICFRTLKLTTPTYGDLNHLVSATMSGVTTCLRFPGQLNADLRKLAVNMVFPRLHFFMPG
β1	FAPLTSRGSQQYRALTVPELTQQMFDAKNMMAACDPRHGRLTVAAIFRGRMSMKEVDEQM
β2	FAPLTSRGSQQYRALTVPELTQQMFDAKNMMAACDPRHGRLTVAAIFRGRMSMKEVDEQM
β1	LNIQKNSSYFVEWIPNNVKTAVCDIPPRG LKMSATFIGNSTAIQELFKRI
β2	LNIQKNSSFFVEWIPNNCKTAVCDIPPRG LKMSATFIGNSTAIQELFKRV

Figure 14. Comparison of the drug binding domain, amino acids 206-381, of β1 and β2 tubulin. Out of the 175 amino acids of the domain, there are 4 amino acid differences.

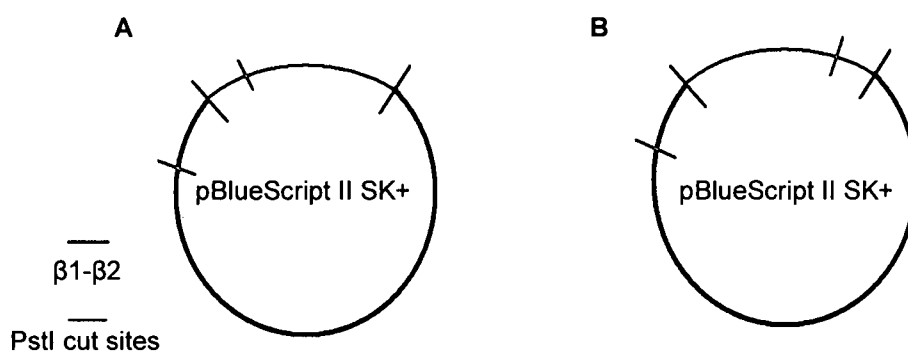


Figure 15. Location of *Pst*I restriction enzyme cut sites in pBlueScript II SK+ in relation to the two possible orientations of the chimeric $\beta 1\text{-}\beta 2$ insert.

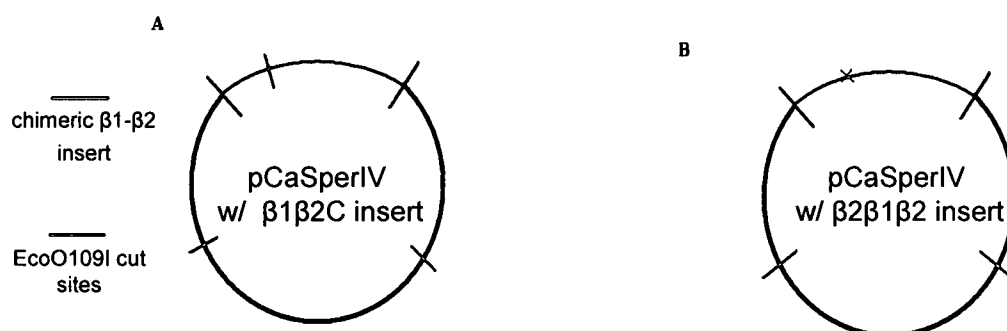


Figure 16. Location of *EcoO109I* enonuclease restriction enzyme cut sites in (A) pCaSpeRIV + $\beta 1\beta 2C$ and (B) pCaSpeRIV + $\beta 2\beta 1\beta 2$.

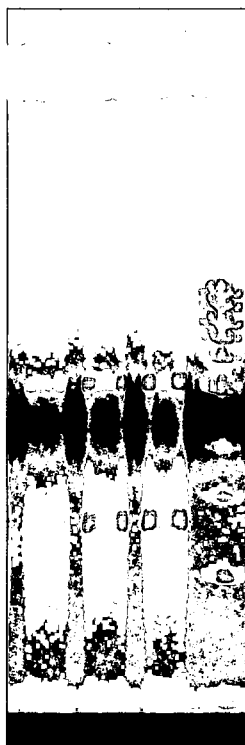


Figure 17. *PstI* restriction digest of pBlueScript II SK+ $\beta 1\beta 2C$ mutagenesis reaction. Based on the size of the two bands of DNA, the orientation of the insert can be determined.

Intron

GCC SGG CAC CAT ^GTAAGTTTTGGGGGATTGGGAATTTATCTGAAAAAGTTTACCCTAC
P G T M

TTTTCTCCAACAG^GGA CTC TGT GCG
D S V R

Figure 18. Fifty-nine base pair intron sequence located between Met 73 and Asp 74 of $\beta 1\beta 2C$.

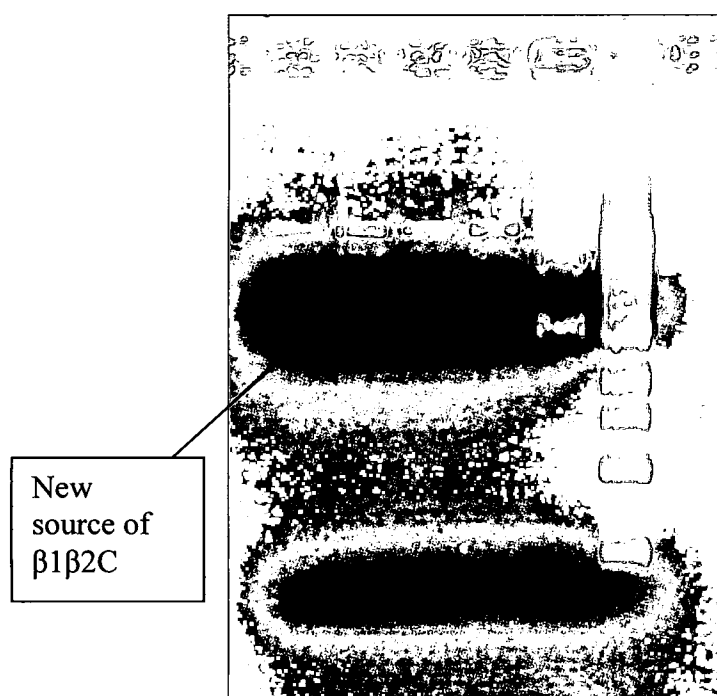


Figure 19. Agarose gel analysis of five potential new sources of $\beta 1\beta 2C$ to replace the previous intron containing $\beta 1\beta 2C$ insert.

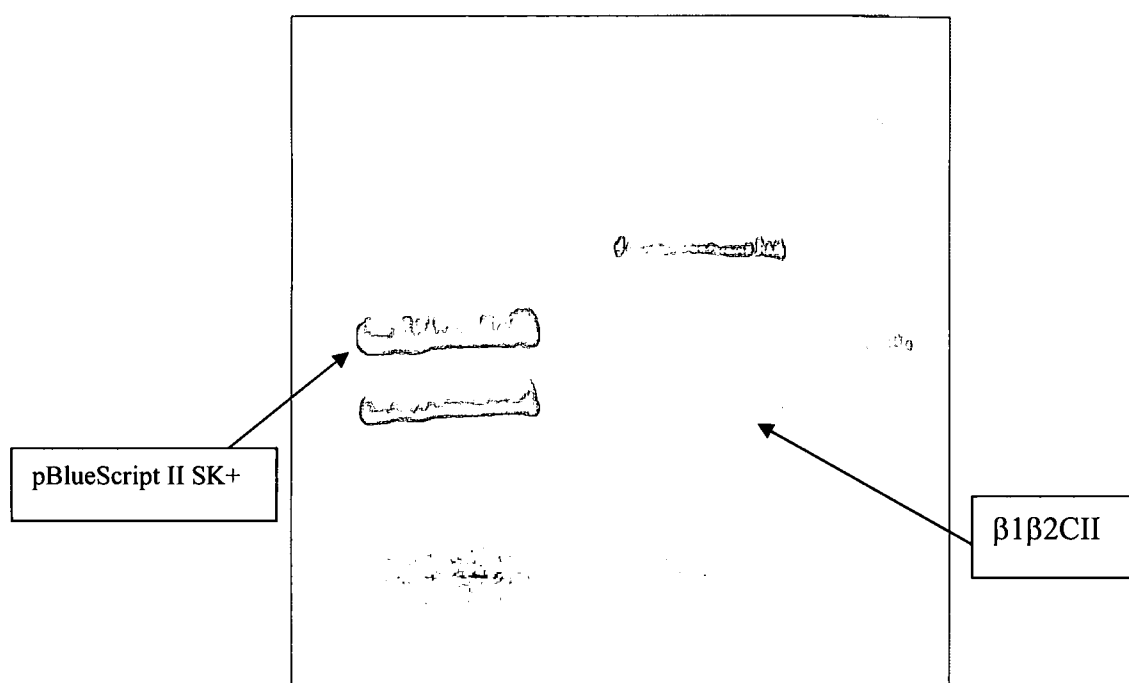


Figure 20. *EcoRI* digest of pCaSpeRIV + $\beta 1\beta 2$ CII and pBlueScript II SK+ containing the original $\beta 1\beta 2$ CII + intron insert. The DNA bands corresponding to pBlueScript II SK+ and $\beta 1\beta 2$ CII were eluted from the gel using the QIAEX II gel extraction kit (Qiagen) and used for subsequent ligation reactions.

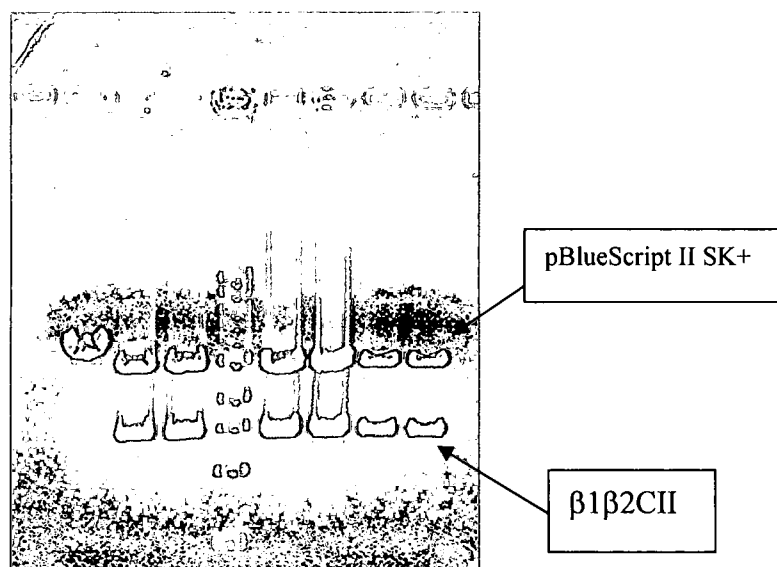


Figure 21. *EcoRI* restriction digests confirming successful ligation of pBlueScript II SK+ DNA - β1β2CII. The 7 samples with inserts were then sent to be sequenced to check for the presence of the 59 base intron in β1β2CII.

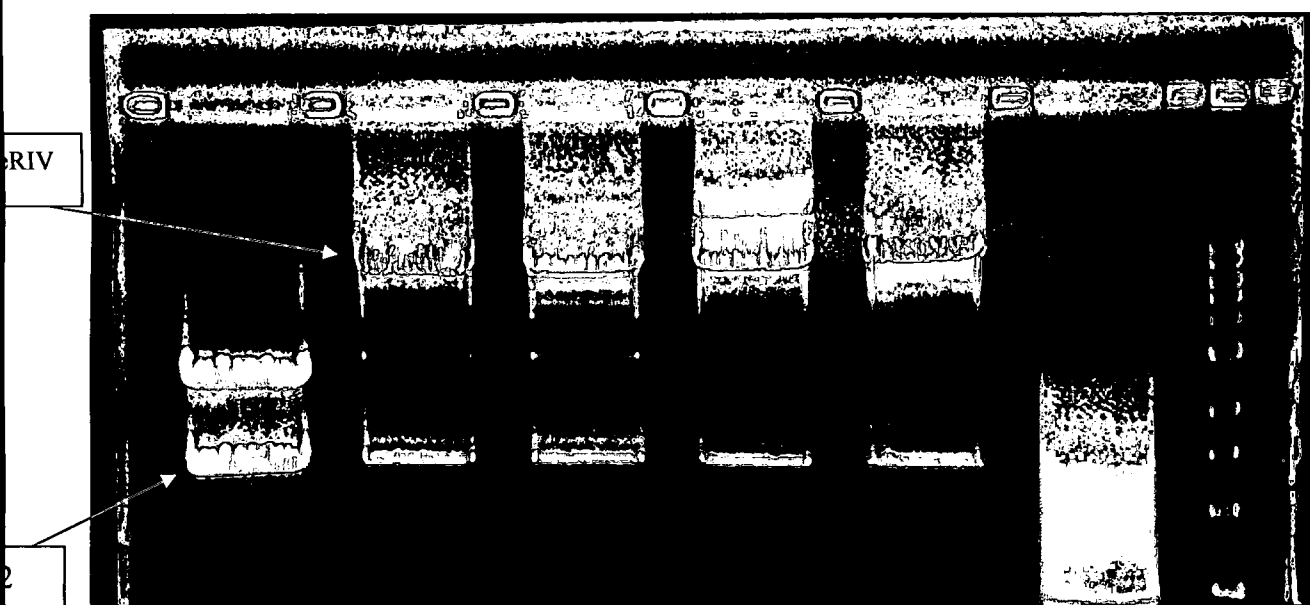


Figure 22. *EcoRI* digest of pCaSpeRIV + β1β2CII and pBlueScript II SK + β2β1β2 insert. The DNA bands corresponding to pCaSpeRIV and β2β1β2 were eluted from the gel using the QIAEX II gel extraction kit (Qiagen) and used for subsequent ligation reactions.

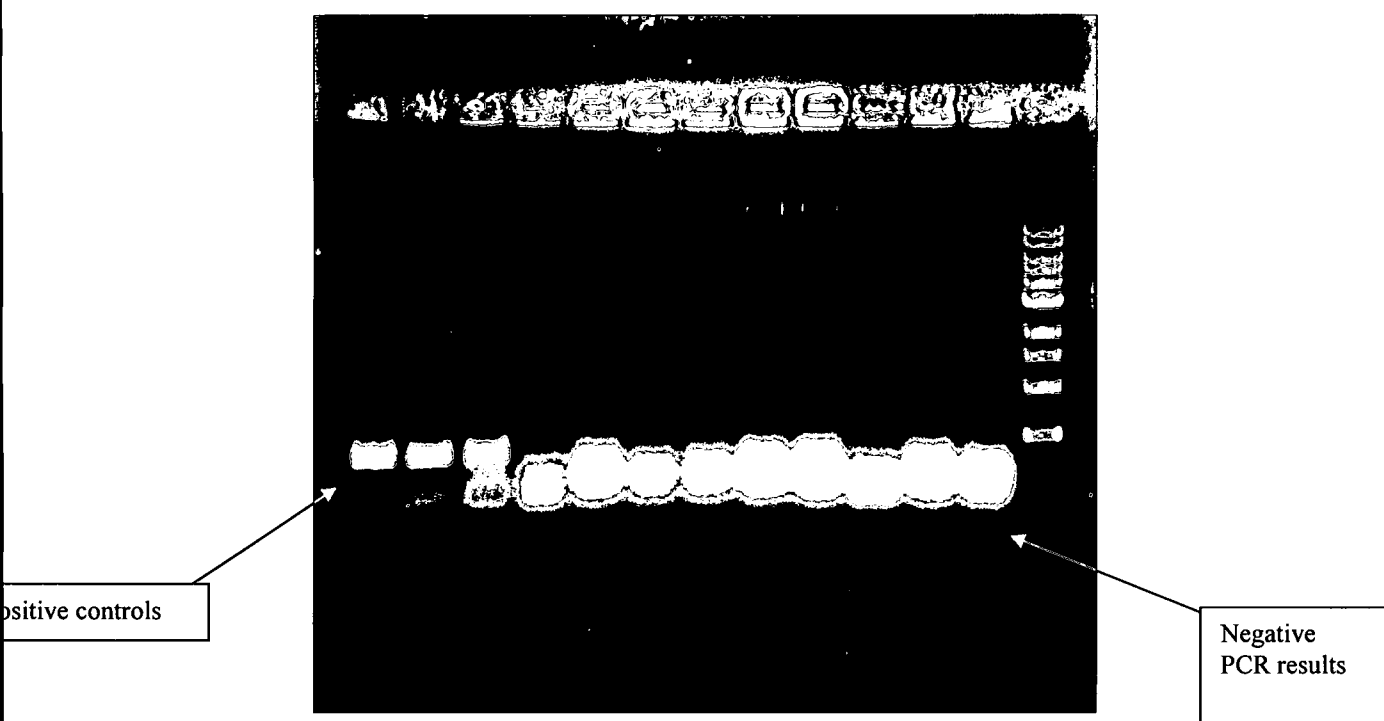


Figure 23. Quick PCR screening method. PCR reaction of nine colonies from a transformed and plated pCaSpeRIV + $\beta 2\beta 1\beta 2$ along with one colony source and two plasmid source positive controls.

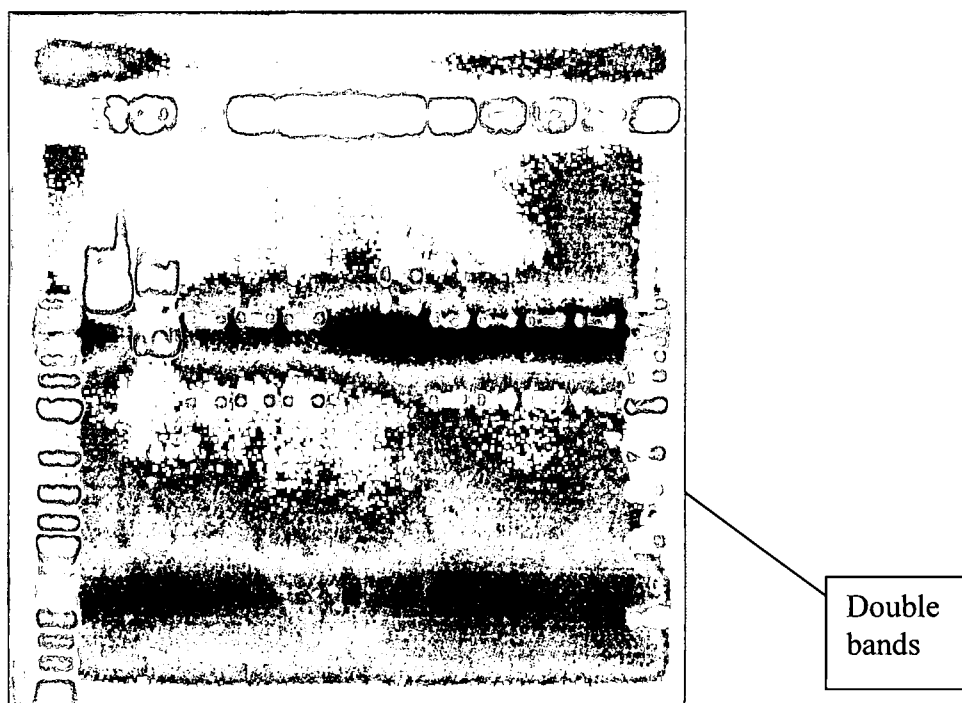


Figure 24. *PstI* restriction endonuclease digest of pCaSpeRIV + $\beta 2\beta 1\beta 2$ ligation. The double bands indicate that there were two cut sites, one within pCaSpeRIV and one within the ligated $\beta 2\beta 1\beta 2$ sequence.

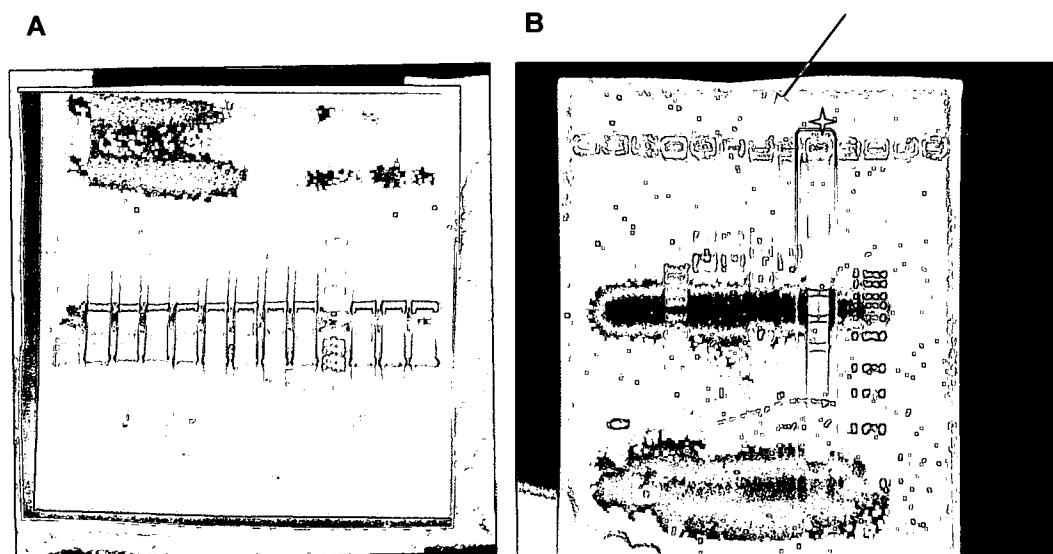


Figure 25. (A) *Eco0109I* restriction endonuclease digest of pCaSpeRIV + $\beta 2\beta 1\beta 2$ ligation. The double bands indicate that there were two cut sites within pCaSpeRIV and none within the ligated $\beta 2\beta 1\beta 2$ sequence. (B) Positive control (indicated by the star and arrow). *Eco0109I* digest of pCaSpeRIV + $\beta 1\beta 2C$ shows three bands, as expected.

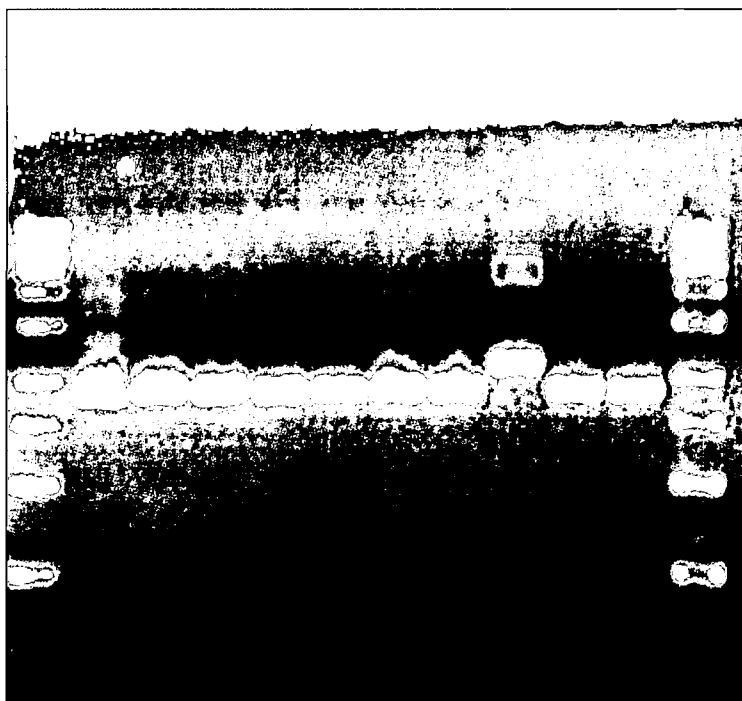


Figure 26. Second domain mutagenesis of $\beta 1\beta 2C$ in pCasper. Size of DNA bands is much too small to be pCaSpeRIV. Vector is too large to perform mutagenesis.

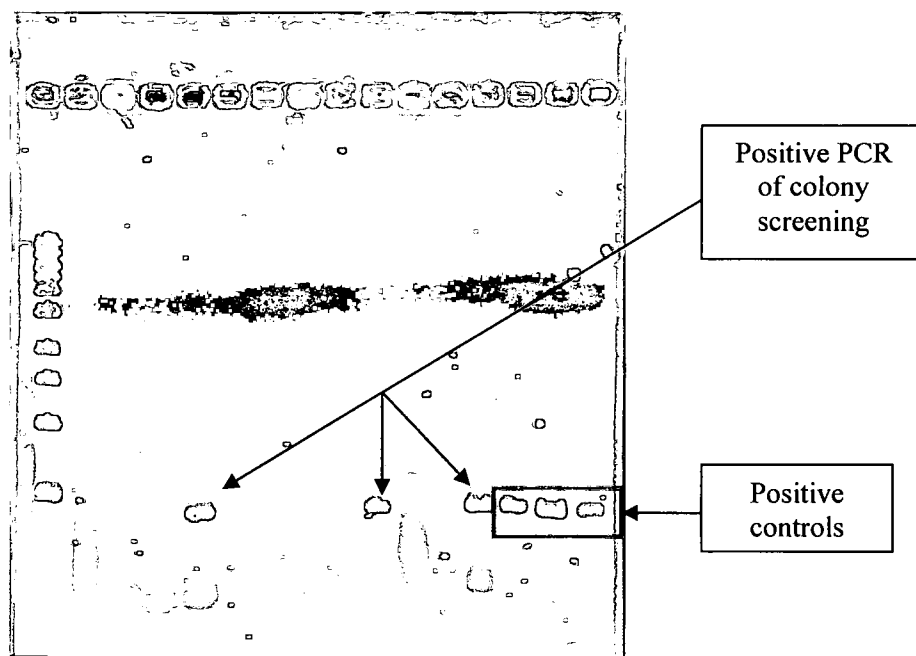


Figure 27. Quick PCR colony screening of pCaSpeRIV + $\beta 2\beta 1\beta 2$ ligation. A positive result for the presence of $\beta 2\beta 1\beta 2$ in three of the samples.

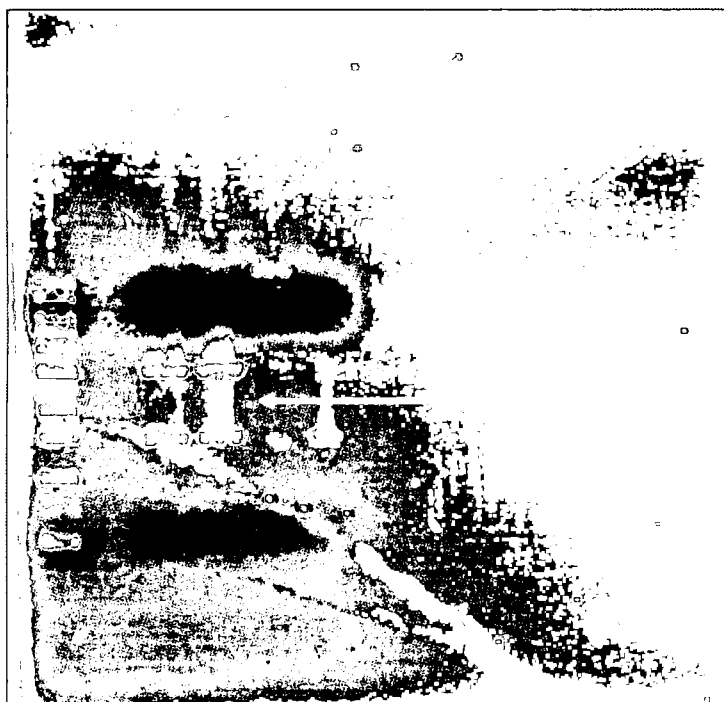


Figure 28. *EcoRI* digest of pCaSperIV + $\beta 1\beta 2\beta 2$. The insert actually is $\beta 2\beta 1\beta 2$, but it is in the incorrect vector, as can be seen by the DNA band of approx. 3kb.

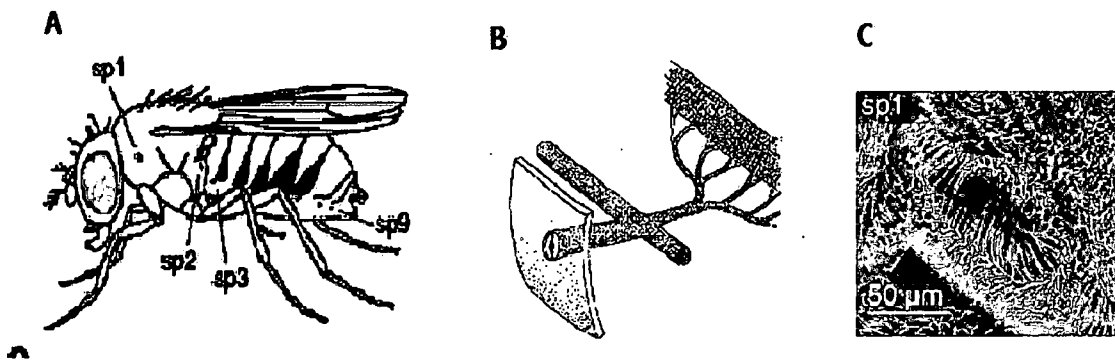


Figure 29. (A) Drosophilid spiracle openings (Lehmann, 2005). (B) Illustration of spiracle opening and branching of the insect tracheal system (D G Mackean, 1988). (C) Scanning electron microscopic image of *Drosophila* spiracle (Lehmann, 2005)

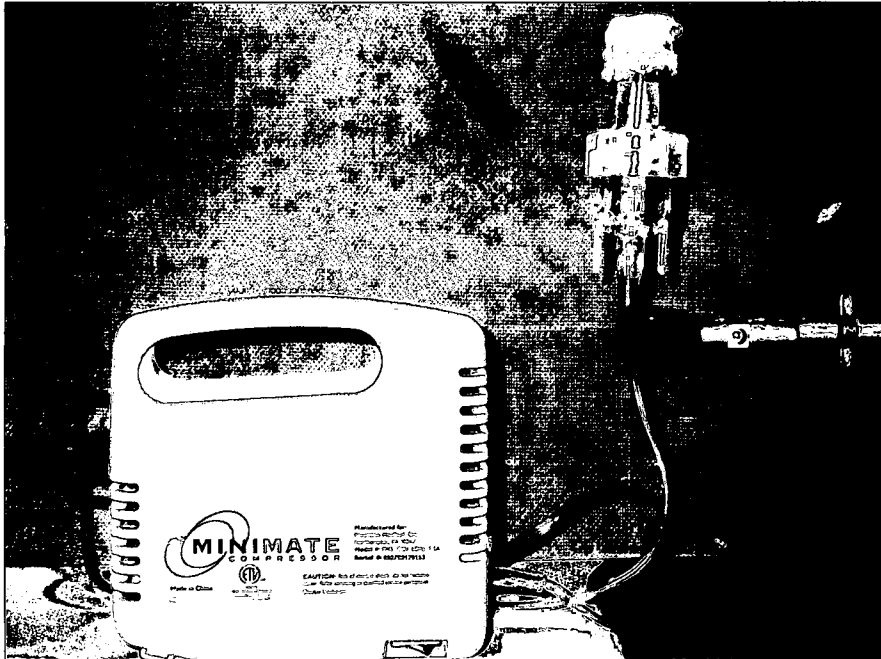


Figure 30. Minimate compressor, model #PM5, Precision Medical, INC. Northampton, PA.
The compressor is attached to the nebulizer and 1 x 3 cm rubber tube chamber.

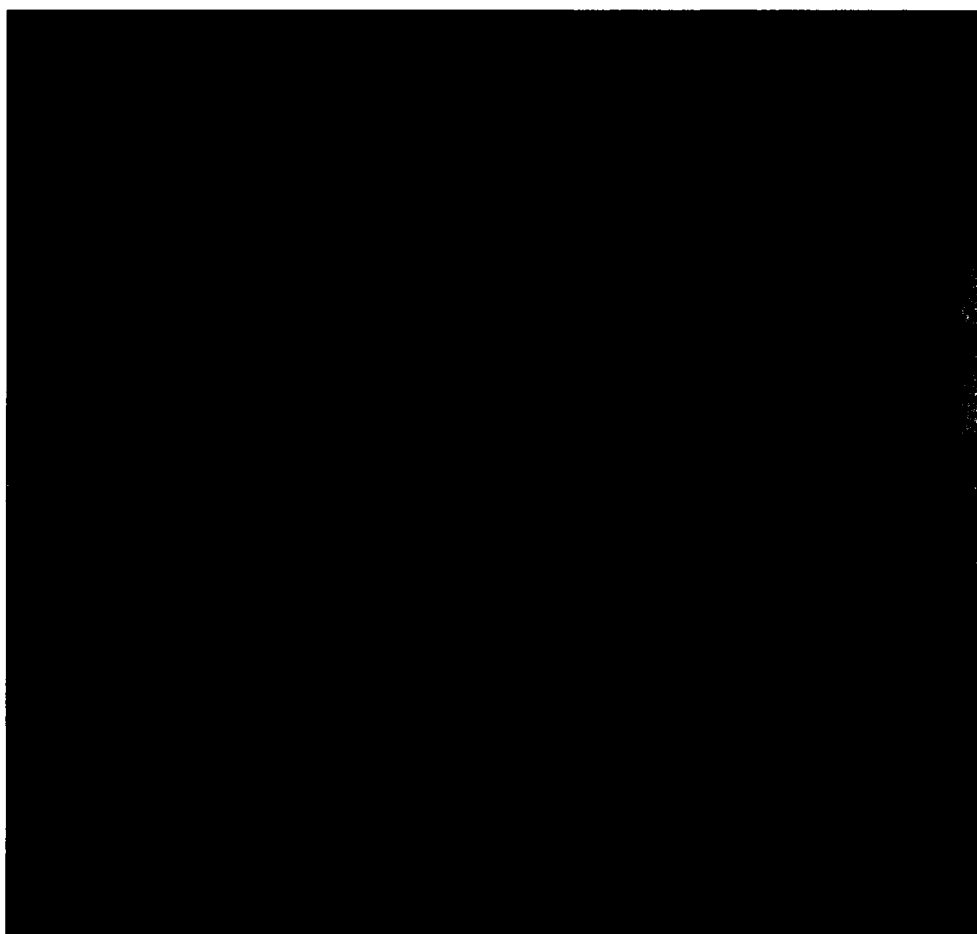
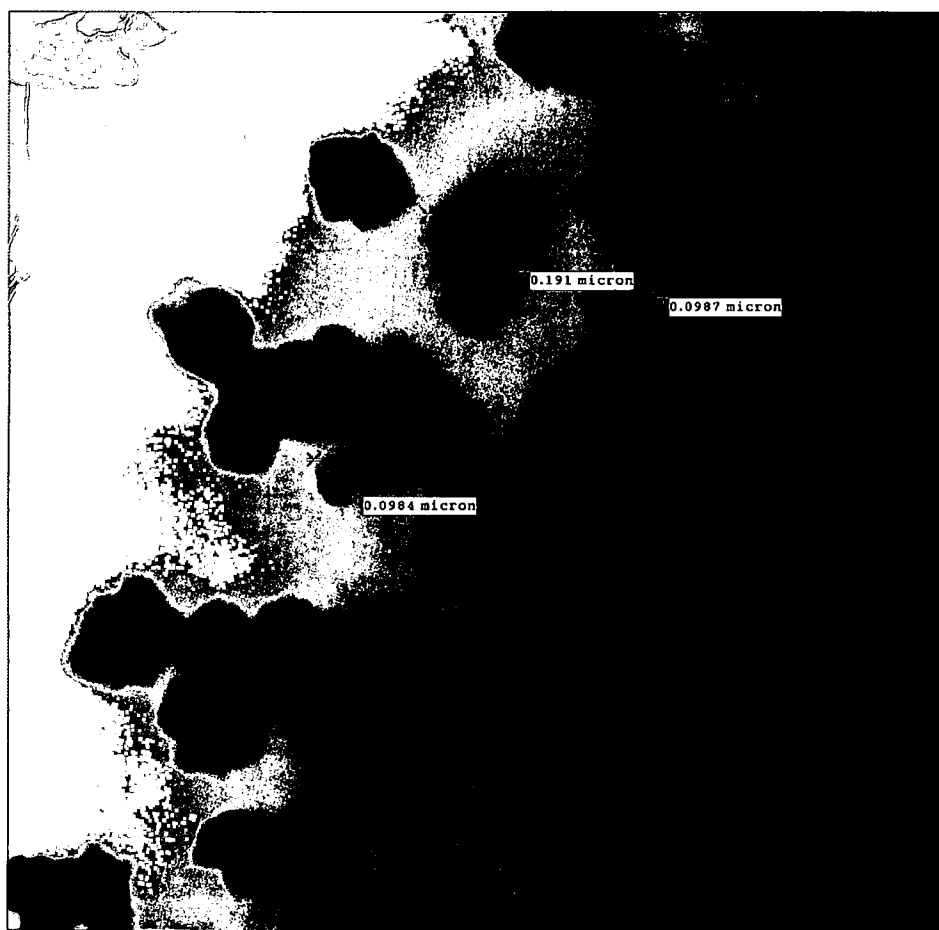


Figure 31. Filter paper exposed to aerosolized 24 nm Fluospheres.



10nm silver in H2O 30km 4-21-08.tif
Print Mag: 111000x @ 7.0 in
15:49 04/21/08
TEM Mode: Imaging

100 nm
HV=100kV
Direct Mag: 30000x
NEST

Figure 32. TEM image of nebulized silver nanoparticles.

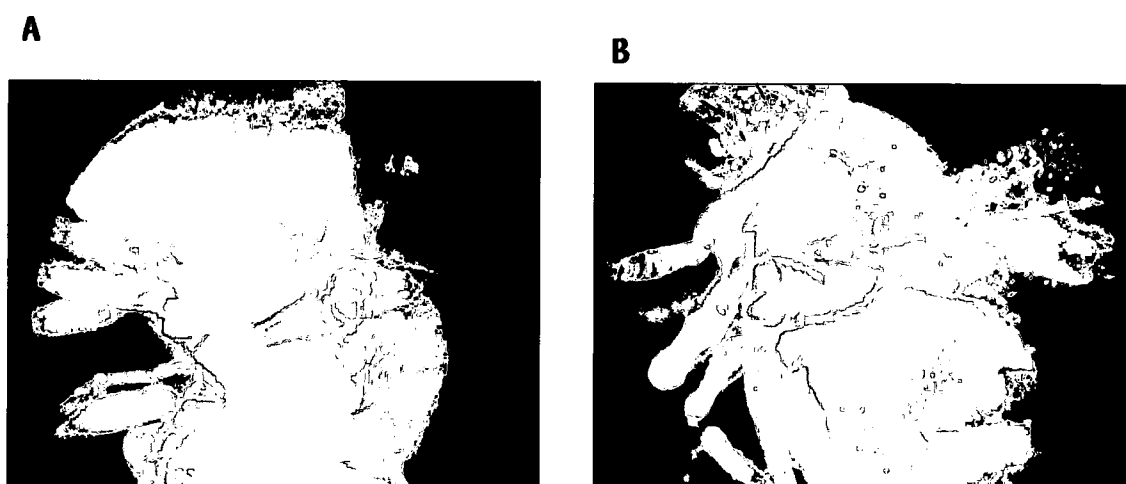


Figure 33. (A) Negative control. Fly exposed to nebulized water only. (B) Fly exposed to 50 $\mu\text{g/mL}$ nebulized CdSe/ZnS quantum dots for five minutes.

Primer 1 a.a. 18, 23, 29	c ggt aac cag atc ggt ggt aaa ttc tgg gag gta atc tcg gat gag cac tgt ata ga G N Q I G G K F W E V I S D E H C I
Primer 2 a.a. 37	c cgg aac cta cta cgg tga cag c G T Y Y G D S
Primer 3 a.a. 55,57,64	ca caa tga ggc gac cgg tgc caa gta cgt gcc ccg cgc tat cct tg Y N E A T G A K Y V P R A I L
Primer 4 a.a. 80	ctc tgt gcg atc ggg agc ttt cgg S V R S G A F
Primer 5 a.a. 124,126,135	g caa gga gtc cga agg ctg cga ctg cct gca agg ctt cca act cac aca ct K E S E G C D C L Q G F Q L T H
Primer 6 a.a. 163,167	ga gta ccc cga cag aat aat gaa cac att ctc ggt tgt E Y P D R I M N T F S V
Primer 7 a.a. 281	ctg aac cat ctt gtc tcc gcg acc L N H L V S A T
Primer 8 a.a. 340,349	cag ctc ctt ctt cgt cga atg gat ccc caa caa ctg taa gac cgc cg S S F F V E W I P N N C K T A
Primer 9 a.a. 381	g ctg ttc aag cgc gtc tcc gag cag ttc acc gc L F K R V S E Q F T

Table 1. Nucleic acid and corresponding amino acid sequences of mutagenic primers for 1st (nucleotide binding) domain: primers 1-6, and 2nd (drug binding) domain: primers 7-9.

RTP1 forward	5' - CTG GAG CGC ATC AAT GTC TA - 3' L E R I N V
RTP2 reverse	5' - CAC TGA GTC CAC CAG CTC AG - 3' F P R L H F

Table 2. Forward and reverse, non-mutagenic, β 1 primers designed to sequence the internal regions of the tubulin gene after site-directed mutagenesis.

R002594018